# CROPLAND AND TREE COVER MAPPING USING SENTINEL-2 DATA IN AN AGROFORESTRY LANDSCAPE, BURKINA FASO

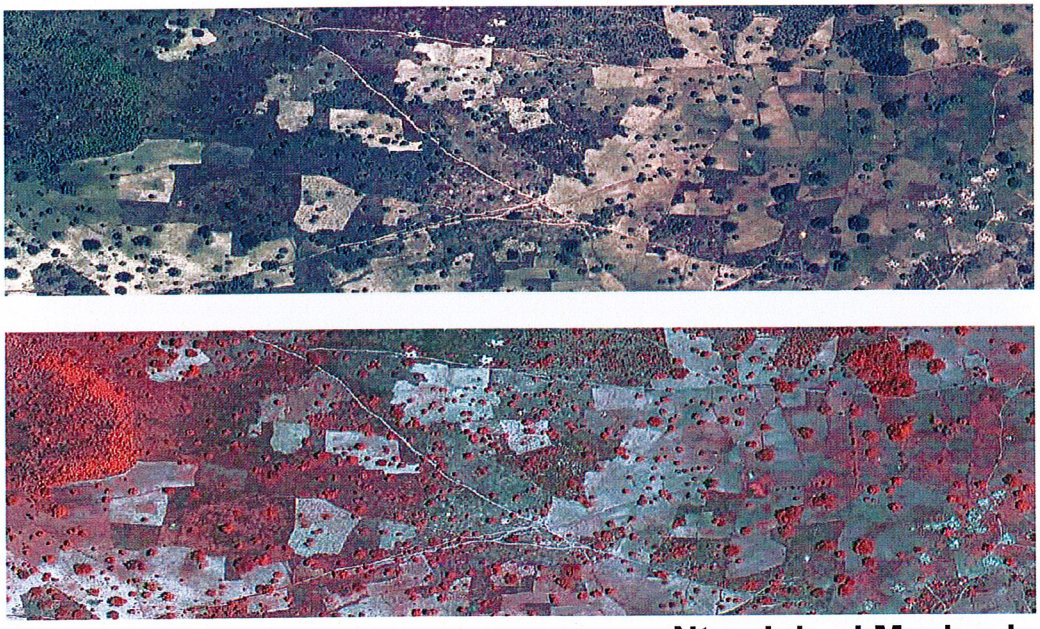

**Ntandokazi Masimula**

**Degree of Master of Science (120 credits)**
**with a major in Earth Sciences**
**60 hec**

**Department of Earth Sciences**
**University of Gothenburg**
**2020 B1097**

Faculty of Science

UNIVERSITY OF GOTHENBURG

**UNIVERSITY OF GOTHENBURG**
**Department of Earth Sciences**
**Geovetarcentrum/Earth Science Centre**

# CROPLAND AND TREE COVER MAPPING USING SENTINEL-2 DATA IN AN AGROFORESTRY LANDSCAPE, BURKINA FASO

**Ntandokazi Masimula**

**ISSN 1400-3821**

**B1097**
**Master of Science (120 credits) thesis**
**Göteborg 2020**

**Mailing address**
Geovetarcentrum
S 405 30 Göteborg

**Address**
Geovetarcentrum
Guldhedsgatan 5A

**Telephone**
031-786 19 56

Geovetarcentrum
Göteborg University
S-405 30 Göteborg
SWEDEN

# Abstract

Sentinel-2, with high spatial resolution bands and increased number of spectral channels, has provided increased capabilities for vegetation mapping. Cropland masks within heterogeneous areas such as the Sudano-Sahel zone have become useful for monitoring landscapes. The objectives of this study were to assess the utility of Sentinel-2 data in classification of cropland for the purpose of creating a cropland mask, and estimation of tree cover. An assessment of the cloud-free, wet season satellite images from 2017 and 2018 (15 in total), from the Saponé agroforestry parkland landscape in Burkina Faso was conducted. The random forest machine learning algorithm is applied to images to perform classification with field-based data as training data, tree crown cover estimation with high resolution Pléiades image and to assess variable importance. The results reveal that due to the dynamic cropping practices, the cropland mask needed to be produced for a single year at a time, and high model accuracy was indicated for 2017 with overall accuracy of 94.7%, yet lower for 2018 (90.9%), even though similar acquisition image dates were used. The best result for 2017 was produced using multi-temporal images from October 7 and 22, while the best result for 2018 was obtained using a single image from October 22. Variable importance measures revealed that the green, NNIR, red, NIR and vegetation red edge5 bands were most important in both 2017 and 2018 analysis. The percent of tree crown cover was estimated for 2017 using Sentinel-2 images from June 29 and October 22 and a random forest regression algorithm. The $R^2$ of the best regression equation was 0.42 with a RMSE of 15.1. The RF prediction had values ranging from 0.52% to 85% tree cover. The relationship between observed and predicted tree cover was linear, however, there was an underestimation of higher percentage tree cover values and an overestimation of very sparse tree cover. Based on the results, Sentinel-2 may be useful for monitoring cropland at landscape level and identifying tree crown cover. However, this study would have benefited from using more discriminating field-based training data (i.e.crop types and harvested fields) to identify active cropland. In conclusion, the Sentinel-2 data, with its 10 m pixels and range of spectral bands in particular the red and vegetation red edge produced good quality cropland masks. The use of high resolution supplementary image (Pléiades) is also recommended as a source of training data for producing cropland masks and tree cover data. The results presented here will contribute to an ongoing research project on the role of trees on agroforestry landscape productivity.



**Keywords: Sentinel-2, Cropland mask, Tree cover estimation, Burkina Faso, Agroforestry, Random Forest**

# Acknowledgements

**Academically**, I thank my advisor Dr Heather Reese, for her continued support and genuine advice on the work and being a part of the research group for this project was an honour, which allowed me to find my feet as a student researcher. Dr Martin Karlson for his co-supervisory support and his work in collecting field data. The project “An integrated approach to explore the unknown role of trees in dryland crop production” is funded by the Swedish National Space Agency thus acknowledgements to them are due as well. Further, I thank the Department of Earth Science and the Biology and Environmental Science for the seminars supporting and keeping our thesis work within the timeline, as well as the space to work with our powerful models.

**My career**, I acknowledge the Swedish Institute for the scholarship, which granted me access to the experience of studies in Sweden and the opportunity to learn from the wide range of experts I have met as I was pursuing my studies.

**Personally**, I would like to appreciate my office mates at Ventifakten, for the coffee, biscuits, the chatter, support, and most importantly the "after works", definitely helped in keeping the spirits high towards the thesis work and life in general. To everyone who supported me especially my wonderful family, lovely friends in Sweden and South Africa.

# Contents

# List of Figures

# List of Tables

# 1
# Introduction

In the past decades, methods have evolved concerning landscape mapping and assessment. The development is seen from aerial photography to satellite imagery, while each is still relevant on its own. Remote sensing methods have developed more with increasing pressure to become freely available, making use of machine learning algorithms (Yang et al., 2019), and automated algorithms for selecting agricultural fields for monitoring. The freely available satellite data from Sentinel-2 with frequent images since 2017 is contributing to agricultural monitoring. The United Nations Sustainable Development Goals (UN SDGs), such as Zero hunger, Life on land and No poverty are key goals that can be monitored with agricultural data collected from earth observation technology (satellites and remote sensing). Using remote sensing data with machine/deep learning algorithms and artificial intelligence enhances agricultural monitoring at different temporal and spatial scales (Fritz et al., 2013).

This project explores the capabilities of Sentinel-2 in relation to creating cropland masks and estimating tree cover within a heterogeneous Sudano-Sahelian agroforestry landscape. Cropland masks and tree cover are an important component towards landscape productivity and land cover/use mapping. Accurate landscape level cropland masks and tree cover estimation leads to accurate national and global monitoring of cropland and tree cover.

## 1.1 Global agricultural monitoring

Agricultural monitoring is currently a major contributor to food security and sustainable food systems (Waldner et al., 2015). West Africa is currently under great threat from climate change, and outbreaks that target crops, affecting food security. Hence, there is a pivotal nature of accurate and timely landscape monitoring and mapping in the region. The Sudano-Sahelian Zone (SSZ), part of West Africa, has land use change on top of

climate change as a driving force of landscape change (Maranz, 2009). Climate change and livelihood vulnerability are some of the defining characteristics of the region. Taking this into account, agriculture is the largest contributor to livelihoods and economic growth in many developing countries which fall within the SSZ. In the recent decade, the growing need to reliably estimate yield and ensure food secure countries globally has increased (Fritz et al., 2019). Increased concerns on how to go about accurate and timely monitoring of landscapes outside of traditional, on the ground landscape monitoring descended into integration of fields such as remote sensing. A perfect example for this integration is the Sen2Agri system developed by the European Space Agency (ESA) Sentinel-2 mission. The system aims to provide high resolution products for crop monitoring from local to national scale (ESA, 2019). Thus, highlighting the critical need for agricultural field mapping for accurate management and policy interventions for many countries within the SSZ.

Cropland mapping can be implemented from a global to a landscape perspective. Global mapping has advantages of a general dissemination of information and knowledge sharing approach for global and national corporation (Fritz et al., 2013), whereas landscape level cropland monitoring, may include high detail information coupled with extensive field work. Remote sensing provides an added advantage and alternative with less time consuming and more repeatable results. Remote sensing has challenges, like many other methods, such as the inability to determine indirect causes of land use/cover change causes such as agricultural practises, land tenure, governance and management (Maranz, 2009). At the same time, remote sensing methods have become an integral part of landscape level vegetation studies.

The areas found within the SSZ zone are defined as parklands due to the integration of agroforestry practices, cropland fields, plantations and grasslands (Maranz, 2009).The SSZ region is heavily researched due to desertification and climate change, which can be directly measured with vegetation studies. The complex variety of agro-ecosystems in the SSZ results in misclassification/identification of agricultural plots in global mapping, and even regional mapping (Defourny et al., 2019). Recently, machine learning and artificial intelligence has proven to provide strong tools for global agriculture, environmental, and vegetation research (Fritz et al., 2019). The way technology is currently used to monitor agriculture includes; automatic crop monitoring with drones, food security apps, and satellite imagery-based global crop health monitoring (Matton et al., 2015;Waldner et al., 2015). Hence, the importance for continued mapping and assessment of satellite based imagery and machine learning from global agricultural monitoring to landscape levels.

## 1.2 The Sudano-Sahelian Zone

The vast Sudano-Sahelian zone, mainly characterised by a semi-arid climate, parklands and agroforestry has become one of the important areas for food security concerns due to environmental changes. This region has gained interest in terms of environmental research that involves the debate of desertification and due to its sensitive nature towards vegetation dynamics, climate change, land-use systems and its location to the south and as a border of the great Sahara desert. Karlson et al., 2016, explores the use of remote sensing in the region for the benefit of vegetation and land use change research. The number of papers published has increased where they make use of remote sensing for observing vegetation in the Sudano-Sahel zone (Karlson & Ostwald, 2016). The region is called the Sudano-Sahel due to the positioning of the area within the African continent. The area represents the transitioning of the dry Sahel region into the wet Sudano region of the equator. The zone is characterised by woody vegetation with patches of grassland, shrubs and agricultural fields.

Burkina Faso lies on the West end of the SSZ zone which stretches from the East to the West of Africa. Though there is uniformity within this latitude, huge differences still exist among different borders. The parklands found within Burkina Faso are a priority area for cropland mapping (Waldner et al., 2015), due to the increasing threats on the landscape. Some of these threats involve a reduction in tree density through cutting down of non-productive trees. Trees are considered an essential part of the SSZ parklands (Waldner et al., 2015), thus taking away essential vegetation within a landscape could lead to breakdown of an ecosystem. Research suggests that due to the trees in the SSZ parklands, their removal could interfere with crops and groundwater. Bargués Tobella et al., 2014 points out the impact trees have in groundwater recharge in dryland areas due to better soil hydraulics in areas with trees. Research such as Waldner et al., 2015 suggests the understanding of tree-crop interactions as critical for management of agroforestry parklands, as they face a decline in area and productivity as a landscape, is rightfully mentioned. Tree cover has become important in terms of climate change and for this particular landscape, for livelihoods and the production of the landscape, it has also become a key variable in vegetation mapping (Karlson et al., 2015).

The region as a whole has a number of challenges. In this regard, Tong et al., 2020 points out the importance of fallow fields in the Sudano-Sahel ecotone and how the fallow fields are often overlooked in studies mapping land cover. These fallow fields are cropland areas which are left fallow, due to tenure and livelihood access (Tong et al., 2020; Knauer et al.,

2017. Ilstedt et al., 2016 and Bargués Tobella et al., 2014, looks at how moderate tree cover in dry or semi-dry regions are important for groundwater recharge. Which can be one of the things that shows how critical research on the role of trees is for dryland landscapes such as the Sudano-Sahel region. In addition, one of the most common tree species in Burkina Faso parklands, *Parkia biglobosa* (African locust bean), is found to have an effect on soil moisture within a parkland in Burkina Faso. Thus, landscape level vegetation studies reinforce natural resource management which heavily relies on cropland harvest forecasts, tree cover estimations, and vegetation health, especially in parkland landscapes.

## 1.3 Capabilities of Sentinel-2

The first Sentinel-2 satellite (2A) was commissioned in 2015 with the second (2B) launched in 2017, and offers essential spectral data for classification of landscapes, leading to land cover/use maps. The Multi-Spectral Instrument (MSI) on board Sentinel-2 offers a huge range of the spectral bands important for vegetation studies especially in the short wave infrared and vegetation red edge spectral bands (Immitzer et al., 2016). A number of studies are riding the wave of machine learning and remote sensing for assessment of vegetation and productivity of landscapes/land use systems. The launch of the Sentinel-2 MSI provides high spatial-resolution images and high revisit time (temporal resolution; Immitzer et al., 2016). Spatial resolution is at 10 m, 20 m and 60 m and has improved spectral configuration with 13 spectral bands in the Visible, Near Infrared (NIR) and Short Wave Infrared (SWIR) regions. Thus, assessing vegetation transition over time, from harvesting to sowing of crop and to cropland plots left fallow, is backed by enough coverage. This revisit time, high spatial resolution and open/free data strengthens decision-making and management in terms of socioeconomic impact of food security, income generation, and to the focus of this paper, land cover classifications and tree cover estimations in relation to parkland practices. Remote sensing in this sense provides a way in which the dynamics of tree-crop interaction becomes adequately evaluated and assessed. Considering the heterogeneity and complexity of the parkland landscapes in the SSZ, it may be challenging for lower resolution satellite imagery, making Sentinel-2 data beneficial (Immitzer et al., 2016).

Xiong et al., 2017 uses Sentinel-2 imagery to address the limitations of remote sensing in the region that encompasses Burkina Faso. Limitations such as the overall accuracy of classification results from different classification methods such as, Pixel-Based and different Object-Based methods. Further, the limitations demonstrated by the Xiong et

al., 2017 study included the presence of clouds within the region and the limited in-situ training data was highlighted for Burkina Faso. Tong et al., 2020 also suggests mapping crops with a per pixel approach. Previous research has established that the capability of Sentinel-2 in the interest of vegetation mapping is the ability to utilise higher resolution 10 m bands for classifications (Frampton et al., 2013 and Immitzer et al., 2016). In addition, the short time of five days Sentinel-2 MSI returns and observes a point on the earths surface speaks to the capability of improving the classification results, especially when using multi-temporal images (Weinmann & Weidner, 2018). However, it has been demonstrated that significant accuracy differences do exist in using multi-temporal versus single images for classifications. Multi-temporal images show better use for classification studies (Weinmann and Weidner, 2018; Karlson et al., 2016; Cetin et al., 2004. Amongst most of the continental region the temporal revisit time for the Sentinel-2 MSI is five days. Thus, without other atmospheric interference such as cloud cover, which is a major contributing factor in the SSZ Xiong et al., 2017, images can be acquired every five days. An increasing number of remote sensing research on land cover classification encourages the use of multi-temporal imagery (Karlson et al., 2014).

The added advantage from Sentinel-2 is the additions in the Short wave infrared (SWIR) and the vegetation red edge (Immitzer et al., 2016). According to Weinmann and Weidner, 2018 spectral channels differ in power for discrimination of vegetation, considering vegetation ecosystem. For example, the Narrow Near Infrared (NNIR), Band 8a on the MSI is much wider with less characteristic nature, therefore the ability to use it for classification diminishes. On the other hand, the red edge bands have confirmed their effectiveness in land classification studies, being a top variable selected for a number of studies within land use and land cover (LULC) vegetation studies (Immitzer et al., 2016;Forkuor et al., 2018; Liu et al., 2016).

In terms of classification methods results using the Sentinel-2 MSI, Valero et al., 2016 obtained, less noisy results visually in the Object-Based with a Post-filtering task classification method. At the same time factors such as the lack of detection of small cropland fields at 20m spatial resolution in SPOT5 Imagery in comparison to Sentinel-2 in conjunction with the 10 m are highlighted as disadvantageous. Several lines of evidence suggest the varying advantages and disadvantages on object based versus pixel based classification, pixel based mapping is said to be more classical than the object based approach (Valero et al., 2016 and Immitzer et al., 2016).

## 1.4 Land cover/use mapping with Remote Sensing

Land Use Land Cover definitions have been a long standing debate, especially when it comes to mapping and reference given to specific LULC. The FAO defines land cover as the observed (bio)physical cover on the earth's surface (Di Gregorio, 2005). On the other hand, land use is the characteristics of the activities pursued within a land cover (Di Gregorio, 2005). Land Use Land Cover (LULC) is important information regarding the landscape, and is a first step towards creating cropland masks. Land cover can be characterised by temporal and spatial differences (Sekertekin et al., 2017).

Present challenges within remote sensing and vegetation mapping include the representation of land cover classes within national and local mapping. For instance, Knauer et al., 2017 points out the challenges of reference data collection in Burkina Faso, where it is difficult to tell the difference between active-cropland and fallow land area due to abandonment or as part of agricultural practices. At the same time unique spectral signatures and developments with season can determine the accuracy of LULC classifications. Due to the nature of the landscape and agricultural practices in Burkina Faso, several land cover classes might be misclassified. However, Foody and Mathur, 2006 explores the accuracy of classifications with spectral mixing and how these might not affect the overall classification of the land cover classifications.

### 1.4.1 Crop land mapping

The main motivation of mapping agricultural landscape is the uncertainty in food security issues globally and especially regionally. It is no doubt that agricultural systems are different around the world, thus making it complex to monitor croplands due to the varying nature of the croplands in terms of management and practices that includes field sizes and crop types (Xiong et al., 2017). High resolution satellite imagery such as the Sentinel-2 provides a tool for better vegetation mapping with the presence of the vegetation red edge bands (Frampton et al., 2013; Forkuor et al., 2018).

A number of discrepancies have been raised concerning the definition of what qualifies as cropland. Due to its importance, cropland is integrated in all existing land cover typologies. The general definition adopted in a remote sensing perspective is

> "...a piece of land of a minimum 0.25 ha (minimum width of 30 m) that is sowed/planted and harvestable at least once within the 12 months after the sowing/planting date. The annual cropland produces an herbaceous cover

> and is sometimes combined with some tree or woody vegetation..." - Joint Experiment of Crop Assessment and Monitoring *(JECAM, 2018)*.

The definition is widely used among cropland research studies. Valero et al., 2016, also created a cropland mask using a plot size minimum of 0.25 ha, thus in line with the JECAM guidelines definition.

Taking into consideration the complexities of the agro-ecosystem found within parklands, a cropland definition with the 0,25ha size definition may be limiting for Burkina Faso parklands. The nature of the landscape comprises of tree cover and tree shadows limiting the coverage of crop plots which may fall under large tree canopies (Valero et al., 2016). Considering that this paper has a study area in a similar landscape, identifying a minimum size of 0.25 ha will be a large limitation for the current project using Sentinel-2 data. However, the use of higher spatial resolution imagery would mitigate this problem in the technical sense but a large disadvantage of that approach is that high-resolution imagery is costly.

A recent study by Tong et al., 2020 puts emphasis on the importance of fallow land cover within cropland mapping. The dynamic nature of practices and landscape within the Sudano-Sahelian region results in land left fallow as a form of leaving the land to recover from previous harvest. The spectral signature of fallow classes can be very different to cropland fields. Tong et al., 2020 suggests that fallow fields among the Sahel croplands is generally greener than the crop field, due to the encroachment of herbaceous vegetation. Previous studies have reported on challenges with cropland mapping on SSZ agrosystems, for example Lambert et al., 2016 and Vintrou et al., 2012. These studies show how extensive the underlying practices in terms of cropping practices is important for the general mapping. The extent of fallow fields within cropland, there seems to be an increasing percentage of fallow fields compared to croplands within the Sahel region. Which for Tong et al., 2020 study is based mainly on the methods and the accuracy of the initial global cropland map used. There is also a suggestion that the fields left fallow, in terms of cropland are alternatively used for grazing, even though generally, research has mostly highlighted the leaving of cropland fallow due to agricultural practice for regenerating the soil. In contrast, Vintrou et al., 2012 looks at cropland mapping with links from food security systems and importance of remote sensing metrics like the Normalized Difference Vegetation Index (NDVI). A similar study Knauer et al., 2017 also explores the ties of agricultural expansion with population growth in Burkina Faso, urging the need for accurate approaches in establishing land use land cover maps in the country.

Further, Tong et al., 2020 showed results of some of the mapped croplands within their

results did not result in crop yields. This point makes it imperative to consider active cropland mapping with yields and so forth due to food security concerns. While a previous study Lambert et al., 2016 produces a cropland map for the SSZ at 100 km using a different sensor, but recommends the use of the Sentinel-2 as an upcoming sensor with great potential at a spatial resolution of 10 m, but does not mention the importance of active agricultural fields. Thus, in essence the use of fallow fields could result in what could be an agricultural field, being included in maps as fallow for different years.

The creation of cropland mask involve land classifications. The Sen2Agri system creates cropland mask from multi-temporal images within a season which are processed with weighted average. The method approach does not rely on ground truth data. However, Fritz et al., 2013 discusses the need for higher quality of validation data for many African countries in current cropland mask products. Valero et al., 2016 uses a range of methods to create a dynamic cropland mask. The approaches by Valero et al., 2016 involved feature extraction of temporal and statistics of spectral data from the Sentinel-2 and spectral indices. The similarity in these approaches is the increased accuracy of the cropland mask with increased input of images that capture the growth of crops. In another study, Vancutsem et al., 2013 uses existing Land Use Land Cover (LULC) datatset to create a harmonized cropland mask at an African continent scale with resolution at 250 m. In essence, this study reiterates that multiple spatial products can create more accurate cropland masks from the continental to landscape level.

### 1.4.2 Algorithms and data input for vegetation mapping

In the recent decade, several studies have made use of machine learning methods for extracting land cover information in multi-spectral and multi-temporal images (Cetin et al., 2004 and Yang et al., 2019). Machine learning algorithms such as random forest proves to be robust with limitations in both regression and classification. The random forest algorithm is given training samples acquired through field visits or from high resolution images and these are used to train the random forest classifier. There is evidence of increasing multi-sensor analysis for the benefit of vegetation analysis (Cetin et al., 2004), thus strengthening higher temporal resolution for producing cropland maps. For instance, Karlson et al., 2015 was able to get an overall classification accuracy of 83.4% using multi-seasonal data input for agroforestry tree species classification. Additionally, Weinmann and Weidner, 2018 also proves the effectiveness of the RF algorithm with input from multi-temporal Sentinel-2 data.

In general, the uses of cropland mapping, tree cover estimations and land cover classifica-

tions include inputs from crop models, management decision making as well as economic statistics (Immitzer et al., 2016). Therefore, satellite imagery like the Sentinel-2 can produce much needed cropland products for the monitoring of landscapes within developing countries in the SSZ.

## 1.5 Aim and Objectives

The aim of this thesis is to determine the capabilities of Sentinel-2 imagery for creating a cropland mask and estimating tree crown cover in Saponé parkland, Burkina Faso. The aim is explored with the following objectives:

1. Test the capability of Sentinel-2 MSI data (spectral bands as variables and different satellite image dates) for accurate land cover classification in an agroforestry parkland landscape, with the end-product being a cropland mask.

2. Investigate the potential of Sentinel-2 MSI data for estimating percent tree cover by upscaling from high-resolution Pléiades data, in an agroforestry parkland landscape

# 2
# Methods and Materials

This section will present the study area information with a visual map of the Sudano-Sahel and the location of the Saponé landscape in Burkina Faso, satellite and ancillary data collection, data analysis workflow, tree cover estimation and accuracy assessment approaches.

## 2.1 Study area

The 10 km x 10 km Saponé parkland study area (Figure 2.1) is located 35 km south of Ouagadougou, the Burkina Faso capital, and lies at N 12°04.48′, W 01°34.00′, with an average elevation of 200 m. The area is landlocked within the Sudano-Sahelian zone (SSZ) of West Africa, which is characterised by a semi-arid climate and scattered woody vegetation. The SSZ is formally referred to as an agro-ecological zone, which lies in the transition zone of the wet region towards the equator (Sudano) and dry Sahara to the north (Sahel; Karlson and Ostwald, 2016).

The rainfall patterns of the SSZ which the study area is within, vary spatio-temporally. The relatively short rainy season, where about 80% of the annual precipitation falls between 600-900 mm/year rain occur between June and September (1901-2016 time period; WorldBank, 2020). The rainfall level and soil properties are a major factor on the structure of the dryland vegetation parklands, which is composed of woody vegetation (trees and shrubs), grasslands and cropland. The landscape vegetation is dominated by two common tree species within SSZ parklands and agroforestry landscapes, the *Vitellaria paradoxa* (shea tee) and *Parkia biglobosa* (African locust bean). Prolonged human influence and activities on the landscape is also a major contributor to the landscape structure and vegetation distribution (Maranz, 2009; Knauer et al., 2017).

The total land area of Burkina Faso is 273,600 $Km^2$ with 61000 $Km^2$ of cropland area

(FAO, 2016). Food and Agriculture Organisation(FAO) reports that in 2016 Burkina Faso had 44.23% of the land area as agricultural land and cropland at 0.4% of the land area. The study area consists of rain-fed agricultural fields, agricultural fields left fallow, tree plantations, riparian woodlands, and patches of settlements (Karlson et al., 2014). The cultivated crops include mainly millet, sorghum, maize and legumes. The active versus fallow agricultural field practices have been a distinct characteristic for the local landscape due to climate variability and livelihood factors (Maranz, 2009).

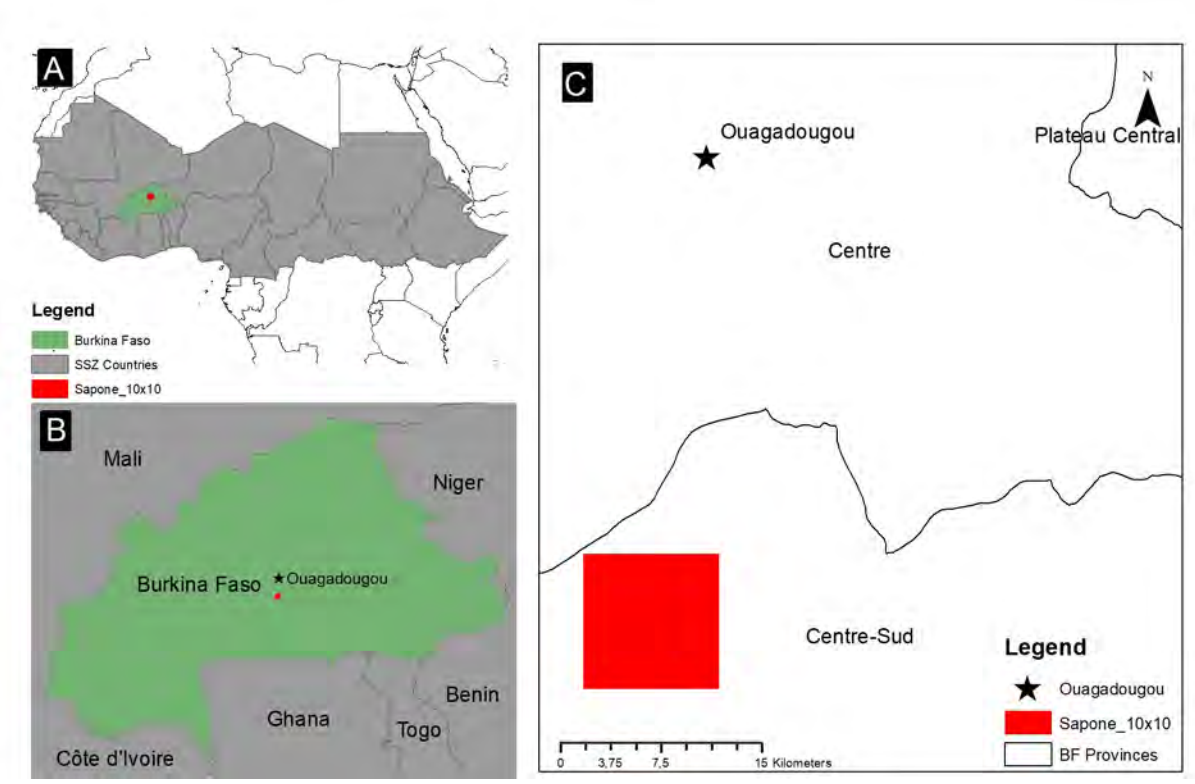


**Figure 2.1:** Location of the study area in Burkina Faso. Location of Saponé landscape (outlined in red). A-Sudano Sahel Zone, B-Burkina Faso, C-Saponé landscape from Burkina Faso capital, Ouagadougou. The large red square represents the satellite image covering the 10 x 10 km study area, and is shown in Figure 2.2.

## 2.2 Satellite and ancillary data

### 2.2.1 Field data

Land cover reference data for this project were previously manually delineated from a 2017 Pléiades image. The reference polygons included land cover attributes and GPS coordinates. The field data contained 488 plots with a size range of 395 to 6769 square metres ($m^2$), which identified land cover attributes, only 210 plots were within the borders

of the Saponé 10x10km study area boundary. Tree reference data was requested from the authors of Karlson et al., 2014 and Karlson et al., 2016 where they had tree crown reference data containing GPS points collected during a 2012 field-inventory with tree species, tree height and tree crown diameter attributes. The GPS points were further used to manually delineate 1148 tree crowns from a WorldView-2 satellite image (from 2012-10-21) with a pixel size of 2m. In this study we used the tree crown data where possible, but also supplemented it with tree crowns digitized from a Pléiades satellite image (from 2017-10-12) with 0.5 m pixel size. The need to supplement with the current Pléiades image was due to the change between 2012 and 2017, where trees present in 2012 were no longer standing in 2017. Each location point is measured using WGS_1984_UTM_Zone_30N coordinate system.

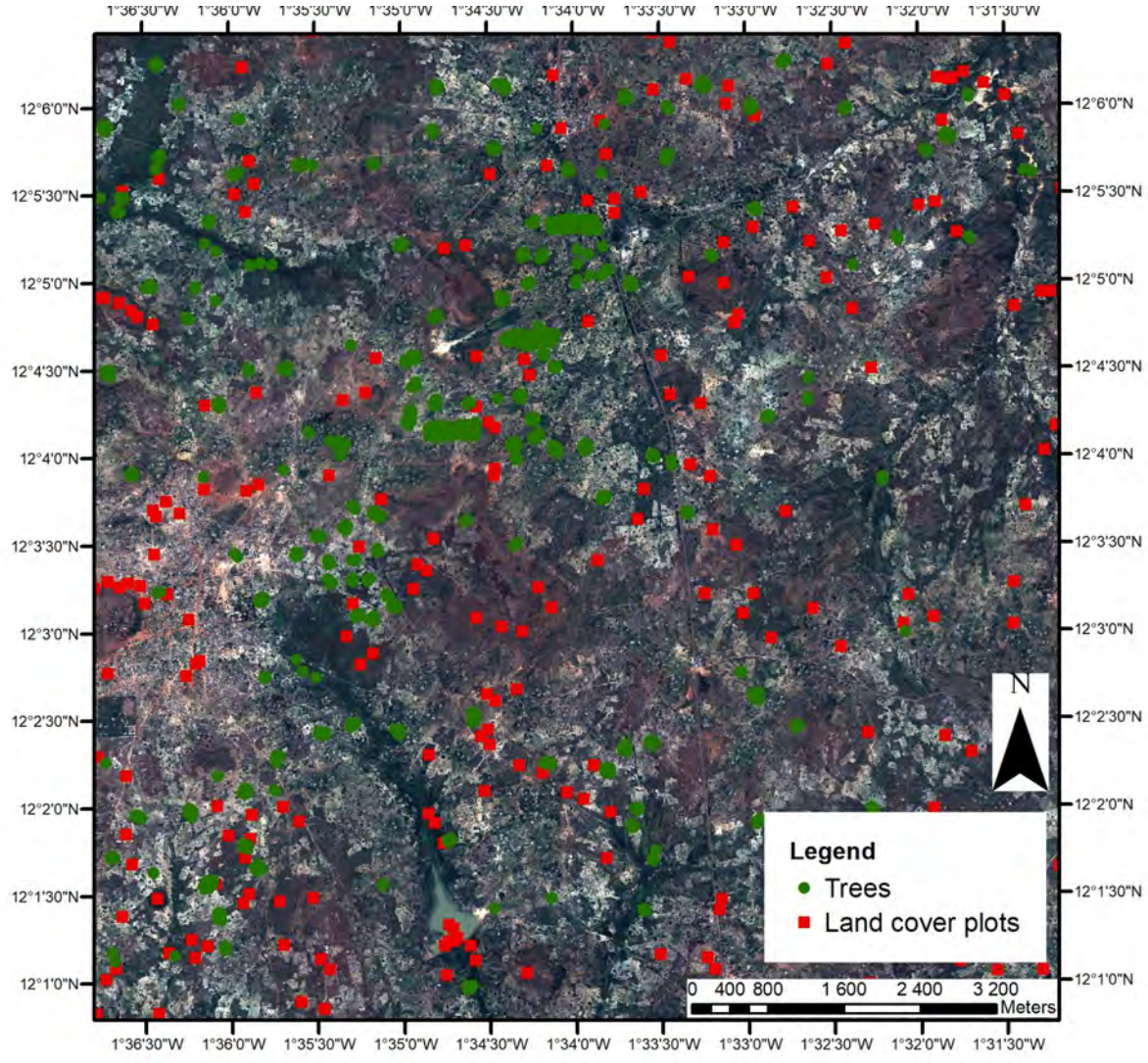


**Figure 2.2:** Location of reference data, with land cover plots and delineated tree crowns in the Saponé landscape. Latitude and Longitude points displayed on true colour Pléiades image.

From the field data points the following are the number of polygons for each land cover class used for training data.

**Table 2.1:** Number of reference polygons and pixels used for training the land cover classifications (Excluding delineated trees).

| **Class** | **Number of polygons** | **Number of pixels** |
|---|---|---|
| Agricultural fields | 54 | 572,274 |
| Tree cover | 38 | 56,274 |
| Bare land | 46 | 30,284 |
| Water | 6 | 3,005 |
| Fallow | 46 | 354,223 |

### 2.2.2 Sentinel-2 MSI data

The Sentinel-2 multi-spectral instrument (MSI) provides 13 spectral bands at 10, 20, and 60 meter spatial resolution and a high revisit time of five days at the Equator (see Table 2.2).

**Table 2.2:** Characteristics of Sentinel-2 and Pléiades bands used in this study. Adopted from the European Space Agency (ESA), Sentinel-2 technical report.

| **Sentinel-2 bands** | **Central wavelength (µm)** | **Resolution (m)** |
|---|---|---|
| Band 1* - Coastal aerosol | 0.443 | 60 |
| Band 2 - Blue | 0.490 | 10 |
| Band 3 - Green | 0.560 | 10 |
| Band 4 - Red | 0.665 | 10 |
| Band 5 - Vegetation red edge | 0.705 | 20 |
| Band 6 - Vegetation red edge | 0.740 | 20 |
| Band 7 - Vegetation red edge | 0.783 | 20 |
| Band 8 - NIR | 0.842 | 10 |
| Band 8A - NIR Narrow | 0.865 | 20 |
| Band 9* - Water vapour | 0.945 | 60 |
| Band 10* - SWIR-Cirrius | 1.375 | 60 |
| Band 11 - SWIR | 1.610 | 20 |
| Band 12 - SWIR | 2.190 | 20 |

All Sentinel-2 images between May to October for the years 2017 and 2018 were considered for this study, with the condition that each image should have less than 10% cloud cover. Cloud cover is a major factor when acquiring satellite imagery. Weinmann and Weidner, 2018, suggests that acquisition at different times of the year should cover phenological variance of the vegetation within a study area. The study area has the image tile identifier of "T30PXU", covering an area of 100x100 km in UTM/WGS84 projection. In total, 15 images from 2017 and 2018 were downloaded from the SciHub platform (see Table 2.3).

**Table 2.3:** Dates of Sentinel-2 images used in this study, with less than 10% cloud cover.

| **Year** | **May** | **June** | **July** | **September** | **October** |
|---|---|---|---|---|---|
| 2017 | 10 | 09 and 29 | 19 and 29 | 07 | 07 and 22 |
| 2018 | - | 14 | 14 and 24 | 17 and 27 | 07 and 22 |

The images were processed at the L1C level, meaning that they have been ortho-rectified and have Top-of-Atmosphere reflectance. Level L2A images were not available via SciHub for this area, and therefore the L1C images were further processed using Sen2cor for

atmospheric and geometric correction (ESA, 2019). ERDAS Imagine software was then used to resample the pixel sizes of the 20 m bands to 10 m using nearest neighbor re-sampling. The 60 m bands (Bands 1, 9 and 10) were removed for the analysis of this study, as they are commonly used for atmospheric correction.

In addition to the spectral band combinations, the Normalized Difference Vegetation Index (NDVI) vegetation index is used as a vegetation phenology parameter (Rouse Jr et al., 1974; Equation 2.1). The NDVI values range from -1 to +1 and vegetation values are generally greater than 0.4 within the NDVI range (Rouse Jr et al., 1974).

$$NDVI = \frac{NIR - Red}{NIR + Red} \tag{2.1}$$

The second index used is the Simple Ratio index (SR), which uses the ratio of the NIR and Red bands (Equation 2.2). The simple ratio has a minimum value of 1, which generally represents bare soils. The ratio has no bounds with the increase in green vegetation within a pixel. It can result in values greater than 15 (Birth & McVey, 1968).

$$SR = \frac{NIR}{Red} \tag{2.2}$$

### 2.2.3 Pléiades data

A Pléiades image with an acquisition date of 12 October 2017 was used for both accuracy assessment in the case of the cropland mask, and training data for tree cover estimation. The Pléiades image has a 0.5 m spatial resolution, and gives higher spatial detail of the landscape. However, it is a commercial satellite, and was not a practical choice of data for operational use over larger areas due to the expense of acquiring more than one image. Pléiades has four spectral bands: Red, Green, Blue and Near-Infrared (Table 2.4). Ground control points from the field and a third order polynomial were used to georeference the image using ArcMap v10.6 software (ESRI, 2020).

**Table 2.4:** Characteristics of Pléiades bands.

| Pléiades bands | Wavelength (nm) | Resolution (m) |
|---|---|---|
| Panchromatic | 480-830 | 0.5 |
| Band - Blue | 430-550 | 0.5 |
| Band - Green | 490-610 | 0.5 |
| Band - Red | 600-720 | 0.5 |
| Band - NIR | 750-950 | 0.5 |

## 2.3 Data analysis

The thesis investigates the utility of Sentinel-2 data for mapping of two different characteristics, namely, a thematic land cover map which will lead to the creation of a crop mask, and estimation of tree cover percent as a continuous variable. The objective is to assess the accuracy of using Sentinel-2 data for these purposes, to identify the best image dates and bands of Sentinel-2 data to achieve higher accuracy, and to create usable maps. Mapping of land cover will be accomplished through classification of the satellite data, while tree cover percent will be done using a prediction model. In both cases, a Random Forest algorithm will be applied.

### 2.3.1 The Random Forest algorithm

The random forest algorithm is a non-parametric technique that uses a bootstrap sample from training data to grow decision trees. Decision trees are the foundation of the random forest model. The decision tree operates as an ensemble independently, therefore it is not correlated with other trees and each tree casts a vote/prediction for the most popular class (Breiman, 1998). While the bootstrap aggregation (sometimes called bagging) is sensitive to the quality of training data, the random forest classifier allows for individual trees to be built from a random sample from the dataset resulting in accurate predictions (Breiman, 1998). It can be used for both thematic classification and prediction of continuous variables.

For classification, Random Forest tends to be more robust and faster. The classifier uses a set number of trees where a subset of the tree is used at random at each iteration (Breiman, 1998). The algorithm has two parameters to function, the number of decision trees (ntree) and the number of variables tested at each split (mtry). The ntree does

not have a limit, but previous studies such as Bolyn et al., 2018, Liu et al., 2016 and Belgiu and Drăguţ, 2016 accept the use of ntree=500 and upwards. The mtry is normally the square root of the number of variables, however, in some instances the mtry can be set to the exact number of variables which could drastically increase computational time (Belgiu & Drăguţ, 2016). One of the capabilities of the RF algorithm is the recursive feature selection based on the leave-one-out cross validation.

Regression can also be implemented using the random forest algorithm to create a continuous data output. The RF regression is popular for the advantage of being able to circumvent overfitting and multicollinearity unlike multiple linear regression (Belgiu & Drăguţ, 2016). Breiman, 1998 states that the random forest for regression, merely grows the decision trees on numerical values instead of class, at the same time random feature selection is used on top of the bagging. Interestingly, the difference in the regression algorithm is the slow increase of collinearity with increased number of features. However, the Random Forest algorithm does not go without limitations, such as the black-box nature of the model or the influence of imbalanced training data (Reese et al., 2014). In this study, the Random Forest algorithm was implemented using the R software R Core Team, 2017 and randomForest package Liaw and Wiener, 2002.

### 2.3.2 Predictor Variables, Variable Importance, and Optimal band combinations

.

Determining variable importance is critical for understanding the input data. The variable importance can be interpreted using the Out of Bag (OOB) error, where the most important variables for the model are chosen due to being the most useful for predicting the most accurate results (Belgiu & Drăguţ, 2016). The random forest algorithm calculates variable importance through prediction error increase when each variables is tested by leaving other variables unchanged (Liaw & Wiener, 2002). Variable importance is capable of selecting the fewest number of predictors that provide the best predictive power. Belgiu and Drăguţ, 2016, reviews the use of RF in remote sensing images, and points out the additional advantage of the internal measurements of variable importance for selecting the best variables for accurate classifications. Variable importance is complex in relation to interaction among variables.

The R software (R Core Team, 2017) is used to check for variable importance ranking given by the package 'varSelRF' (Diaz-Uriarte, 2007). The package does a variable selection from random forests using both backwards variable elimination and selection based on

the importance spectrum. Variable importance can be performed for both classification and regression (using Variable Importance or Variables Selected). Variable importance from the RF algorithm ranks variables according to the mean decrease in accuracy and mean decrease in gini for classification. Different from the RF classifier the regression algorithm produces variable importance as percent of Increase in Mean Squared Error (%IncMSE) and %Increase in Node purity (%IncNodePurity). The %IncMSE is measured from randomly permuted variables resulting in increase in MSE of predictions for each variable. This is considered a robust measure for the RF regression (Freeman et al., 2016). The %IncNodePurity relates to how each split in the decision tree reduces node impurity, the impurity is MSE for regression and gini-impurity for classification. All these measures assess the decision tree purity and accuracy of the variables. For this study, different Sentinel-2 bands are analyzed for variable importance in single and multi-temporal image models. After determining the images which had the best model performances, variable importance was determined.

### 2.3.3 Land cover classification

. The first goal was to make a thematic classification that can be used as an annual crop mask, with five main classes, namely agricultural land, forest, bare land, water and fallow. The land cover classes were kept to a coarse five classes as these were adequate for creating a crop mask, and also due to the field and reference data available. Defourny et al., 2019 argues that keeping the diversity of classes within training data keeps the accuracy of cropland maps fair. Hence, five classes in this study were considered to be diverse enough.

The Saponé 10x10 km boundary is used to clip all images for further analysis, using the clip function on ArcMap. The Sample function in Spatial Analyst is used to extract the spectral values on all bands from all images for 2017 (Table 2.3), and then for 2018, for each point from the training data GPS points. Two radiometric indices were also included: NDVI and SR (Equation 2.1 and 2.2). This results in two tables with all the spectral values for all bands in each year. Figure 2.3 depicts the flow diagram for the methods and detail of image processing.

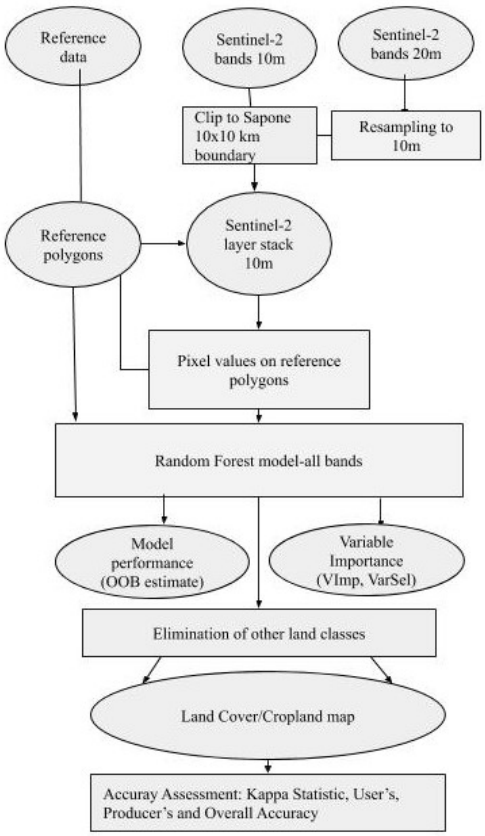


**Figure 2.3:** Overview/Workflow chart of pixel-based classification and validation methodology for land cover mapping

The random forest (RF) algorithm was used to classify land cover using different combinations of the images listed in Table 2.5. It was an objective to determine the best image dates and bands, and therefore the RF algorithm was applied to all images acquired to evaluate and select the images and bands leading to the highest classification accuracies. This was assessed using the OOB error and variable importance from the R software R Core Team, 2017, using the randomForest (Liaw & Wiener, 2002) and varSelRF Diaz-Uriarte, 2007 packages. The following parameters were selected for the RF model: ntree = 2000 and mtry varied with date combinations, using the maximum number of variables available at each run.

**Table 2.5:** List of different image combinations for 2017 and 2018.

| Year | Combined Image dates | Abbreviation |
|---|---|---|
| 2017 | July19_Sept07_ Oct7 | JSO |
| | June29_Oct07_Oct22 | JOO |
| | Oct07_Oct22 | OO |
| | June9_June29_Oct07_Oct22 | JJOO |
| 2018 | Sept27_Oct7_Oct22 | SOO |
| | Sept27_Oct22 | SO |

The cropland mask is generated from the land cover classification results which extracted land cover classes based on spectral data. The best land cover classification is used to create the cropland mask from both the 2017 and 2018 classifications. This required the following: (i) reclassification of the land cover into two classes (cropland and non-cropland) on ArcMap (ii) combination of the tree cover, bare land, water and fallow classes as one.. Furthermore, the importance of definitions was highlighted in the introduction, specifically in terms of cropland. Table 2.6 gives an overview of the definitions of the different classes and other land cover types.

**Table 2.6:** Definition of the different land cover classes used in text and classification.

| Class name | Description |
|---|---|
| Forest | Dry forest, including woodland<br>(Woody vegetation cover including trees and big shrubs) |
| Agricultural fields | Rain-fed vegetation, including plantations and cropland.<br>(JECAM guidelines(2013) definition of 0.25ha minimum size) |
| Fallow | Shrub/grassland like areas not currently used for agriculture<br>(less than five years; FAO, 2015) |
| Bare land | Little to no vegetation, might include buildings |
| Water | Area covered with water |

### 2.3.4 Estimation of percent tree crown cover

The aim of this objective is to determine the role of Sentinel-2 spectral variables in predicting tree crown cover percentage for the 2017 data only. Figure 2.4 depicts the overall steps taken to estimate tree crown cover percentage and area.

Reference data came from manually delineated individual crowns from using a high resolution (2 m) World-View-2 image from 2012 and reference data from a previous study (Karlson et al., 2015). A mismatch of the 2012 tree crown polygons seen against the high resolution Pléiades image from 2017 led to rectification of the World-View-2 delineated polygons, using the Pléiades image. However, due to frequent removal of trees, the delineated polygons were modified by delineating more polygons from the Pléiades image from 2017, which was closer in time to the Sentinel-2 data. Only visually interpretable tree crowns were selected for delineation (Karlson et al., 2015).

There exist multiple ways to estimate tree cover percentage, i.e., multiple linear regression and neural networks. Regression trees are also an appropriate method to determine percent tree cover and have the advantage of being easily interpreted with variables that are continuous (0-100% tree crown cover) and useful for non-linear data relationships (Rokhmatuloh et al., 2005). For these reasons, the Random Forest regression algorithm is used in this study to estimate tree cover. June and October 2017 images are chosen for the tree cover in due to their good classification results. Different variables and models are tested for the optimal model. The algorithm is implemented in the open source R software (R Core Team, 2017), to produce the regression model and variable importance. The same with the RF classifier, the RF regression algorithm also produces internal variable importance. Varsel (varSelRF; Diaz-Uriarte, 2007), is used to test the optimal bands important for predicting tree cover. The selected variables are used for the prediction as optimal variables in an optimal model.

The models were fitted using parameters ntree=2000, mtry varied with date combinations, using the square root of the number of variables. The response and predictor variables for tree cover estimation are summarised, which considered all bands, SR and NDVI for the different image acquisitions and combinations. The random forest regression algorithm modelled the relationship between tree cover percentage as determined by high resolution Pléiades data as the response and spectral reflectance from Sentinel-2 as the predictor. The best models are selected and using the selected variables from the varSelRF results on predictor variables importance, a final predicted tree cover map is produced using the optimal conditions. The resulting map gives a continuous variable which can be interpreted as the percentage of area covered by tree canopy per unit area (one Sentinel-2 $10 \times 10$ m pixel).

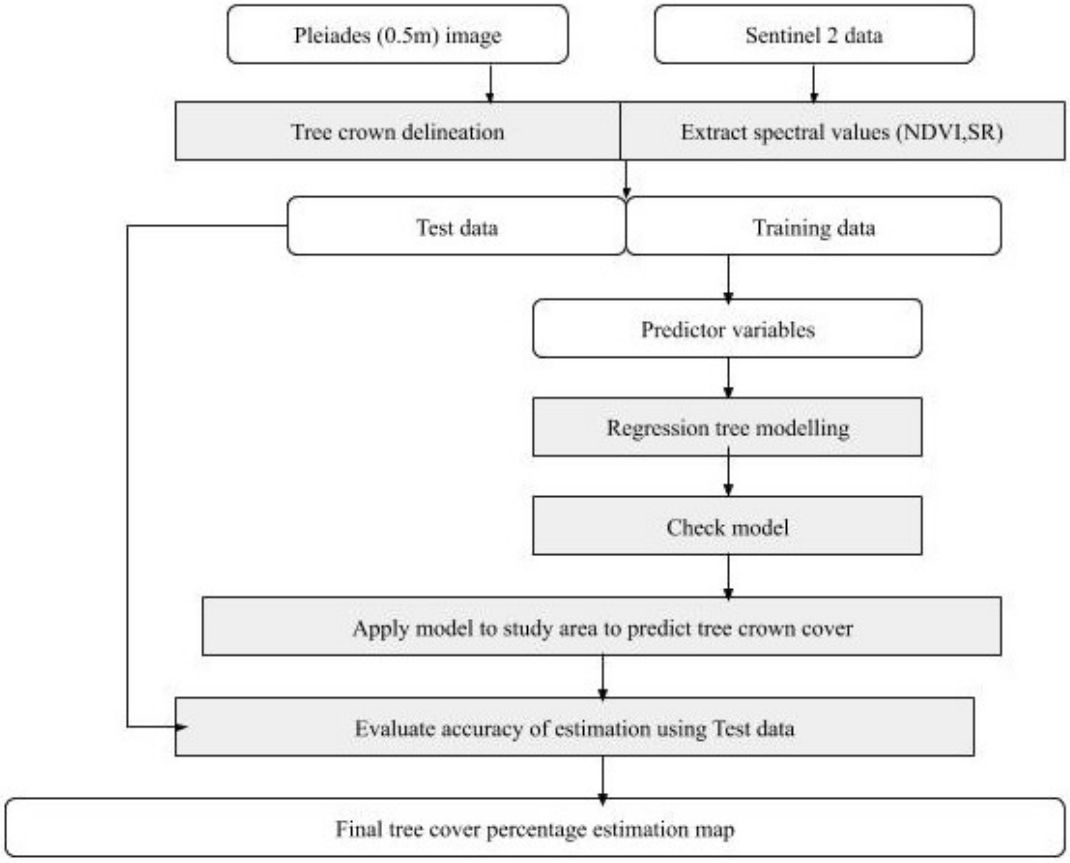


**Figure 2.4:** Workflow for tree cover estimation using Pléiades 0.5m image and Sentinel-2 spectral variables.

## 2.4 Accuracy Assessment

Accuracy assessment is an important step when utilizing remote sensing data. The random forest algorithm produces an out-of-bag (OOB) estimate of error that relates to the model fitness for classification and regression performed. This is an advantage of the random forest algorithm, that it provides a measure of model sensitivity. The OOB error is based on an error of estimate based on training data. The error rate is calculated by prediction of data not found within the bootstrap iteration sample ("out-of-bag" data) and the OOB predictions are combined to give an OOB estimate of the model (Liaw & Wiener, 2002). The OOB error estimate is suggested to be accurate, however, studies utilizing random forest classification and regression do not always report only the OOB error but might also include a k-fold or leave-one-out-cross-validation.

This study uses a permutation test cross-validation for the best Random Forest models

created. Both classification and regression models are run with the rf.crossValidation package. Validation requires high quality reference data independent of training data. Firstly, as a form of assessing the accuracy of the classification, the kappa coefficient is calculated in R Software. The kappa statistic is a popular approach for accuracy assessment in classification studies. In addition, error matrices that include the Overall Accuracy (OA) and Producer's and User's Accuracy (PA and UA) are produced. The cropland mask is assessed with random points on the Pléiades image and Cropland mask, creating a confusion matrix of cropland and non-cropland.

This study will also make use of global cropland cover reports and a dataset to assess if the cropland extent results at the landscape level fits with the national (Burkina Faso) cropland and tree cover extent. One of the reports used is the Climate Change Initiative (CCI) annual land cover maps as final percentages are assessed and discussed (ESA, 2017). Some of the discrepancies experienced involve, different reference year of data, cropland definition (as described in the Introduction, Chapter 1), methods used and resolution of data used to create the national coverage. Most of the cropland and tree cover reported is also derived from global datasets and methods.

# 3
# Results

The results are presented in order of the methods section. This means, the classification results are presented, followed by results for the tree cover estimation. Each result from the objectives is presented, including variable importance, accuracy assessment of models and overall predicted classifications, cropland and tree covers.

## 3.1 Land cover classification

### 3.1.1 Variable Importance

Figure 3.1 shows the model accuracies for each single date images for 2017 (n=8) and 2018 (n=7), as well as a multi-temporal combination of images. For 2017, the single image dates from 2017 with lowest Out-of-bag (OOB) estimate of error rate were June 29 (13.9%,), October 7 (10.16%) and October 22 (8.56%). By combining the two October images as the best single performing images (in terms of model accuracy), into a multi-temporal input for 2017 (OO_2017), a more accurate model could be obtained, yielding an OOB error rate estimate of 5.35%. Adding the third best performing image June 29 on the October images combination (JOO_2017) result in an OOB of 6.95%.

For 2018, the single image dates from 2018 with lowest Out-of-bag (OOB) estimate of error rate were September 27 (13.33%), October 7 (15.24%), and October 22 (8.57%). The best multi-temporal input for 2018 was September 27 and October 22 (SO) and September 27, October 7 and October 22 (SOO), both combinations yielding an OOB error rate estimate of 9.05%. However, as a single date model, October 22 shows a slightly lower OOB error as the multi-temporal combinations for 2018.

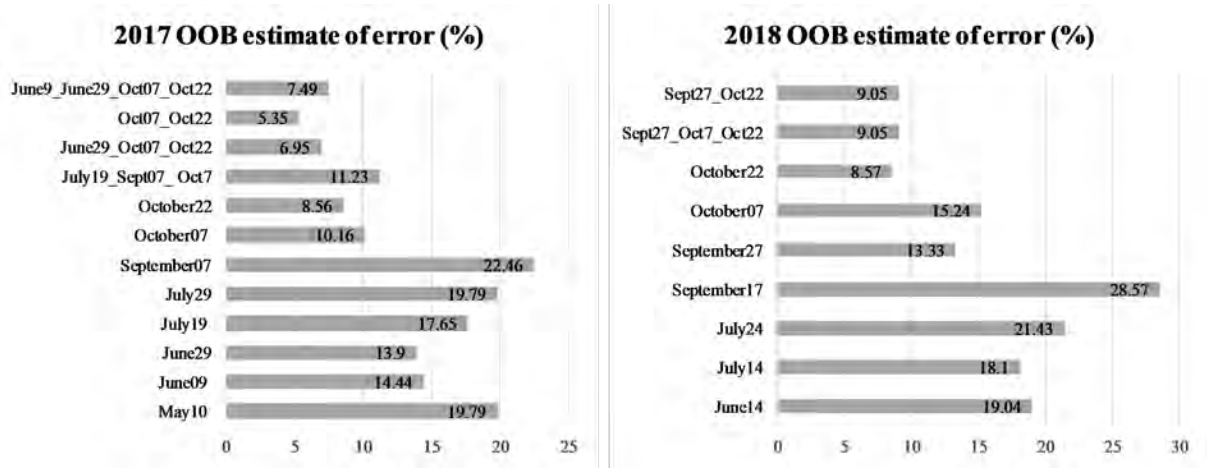


**Figure 3.1:** Out-of-Bag (OOB) error estimate of single and multi-temporal image combinations for 2017 (right) and 2018 (left). Lower OOB error % indicates a more accurate model

Variable importance was inspected for the four single date images with the lowest OOB error, namely June 9 and 29, and October 7 and 22, 2017. The variables in the June images having the largest mean decrease in accuracy (i.e., most influential or important) are the red, narrow near infrared and the shortwave infrared (SWIR) bands, while for the October single date images a higher mean decrease in accuracy is seen for the red, green, near infrared and the red edge bands (see Figure 3.2).

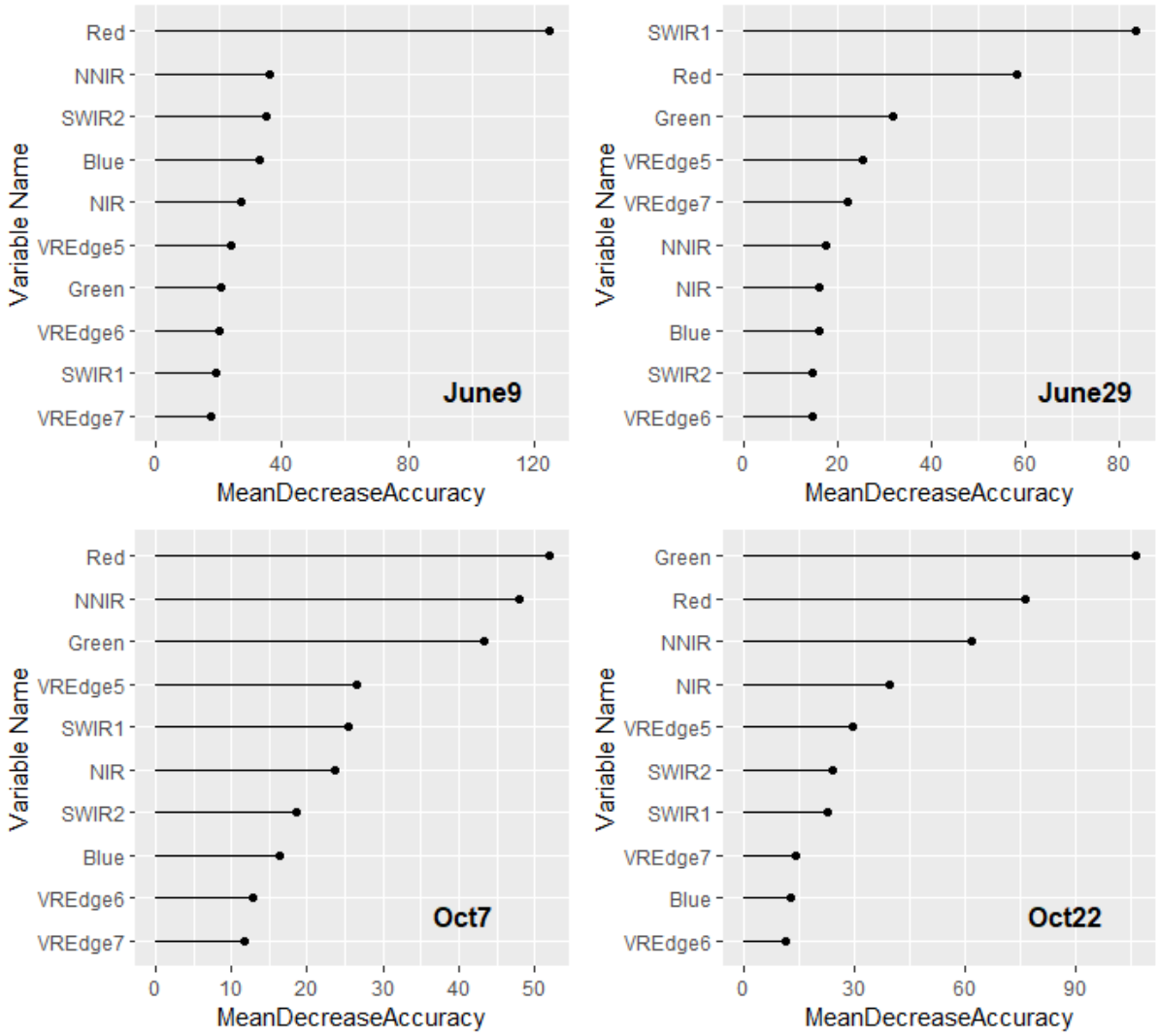


**Figure 3.2:** 2017 Variable importance for the images with the lowest OOB error in the model.

The same variable ranking can be done for the combination of images (multi-temporal models). In the JSO (July19, September7 and October7) combination for 2017, the importance of the October image is clear, with the three highest ranked bands from the October 7 bands having a higher rate of importance than the other bands (Figure 3.3 and 3.4). In the JOO (June 29, October 7, October 22) combination, the June 29 image variables of SWIR and red bands become important in combination with the October images, while the red, green and SWIR bands were important from the October images. For the OO (October 7 and 22) multi-temporal combination with the lowest OOB error, the red, vegetation red edge, and green bands from both dates stick out as important.

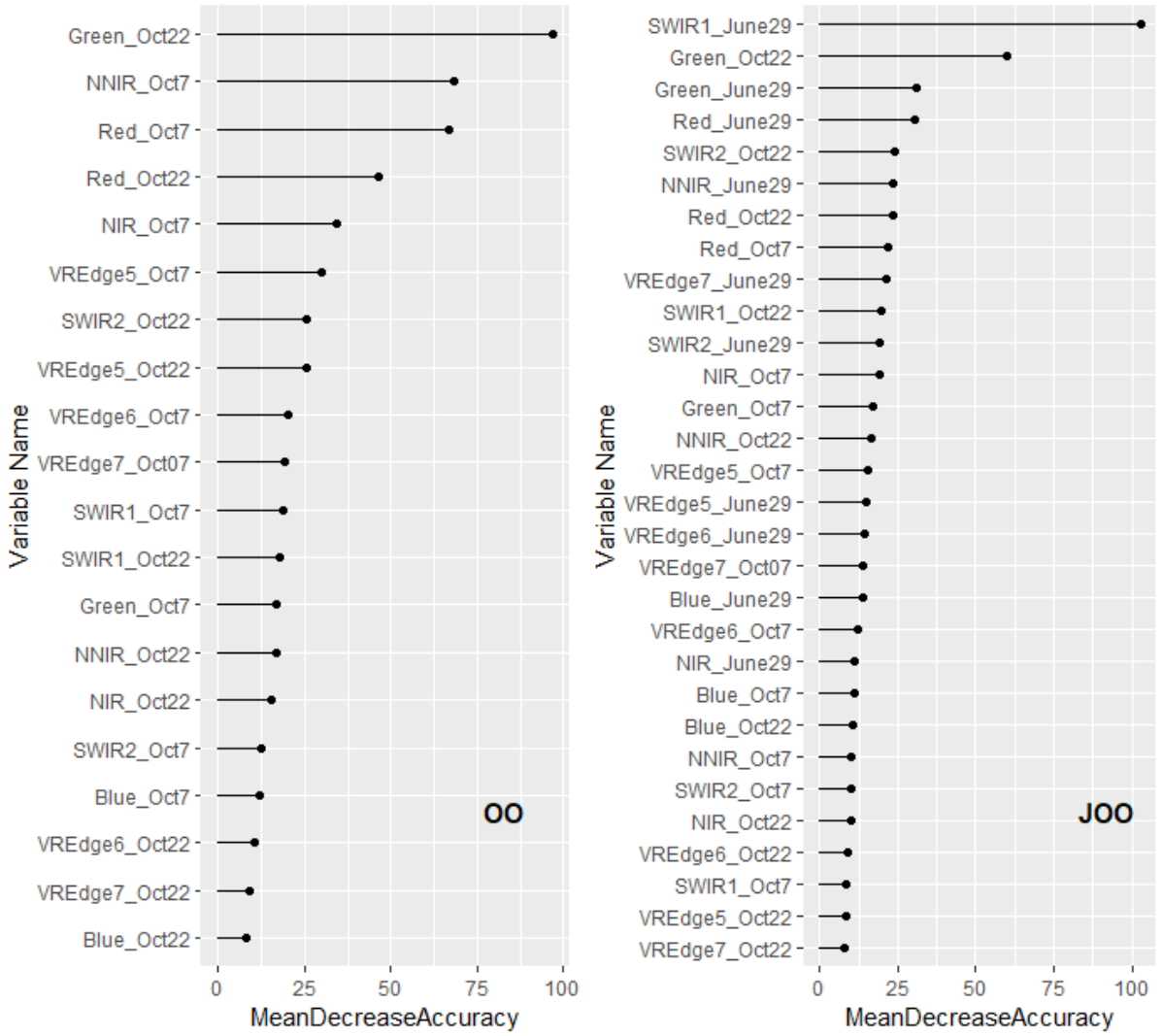


**Figure 3.3:** Variable importance for different combinations of the satellite images according to the variable importance measure from the Random Forest. OO=Oct7 and Oct22; JOO=June29 Oct7 and Oct22

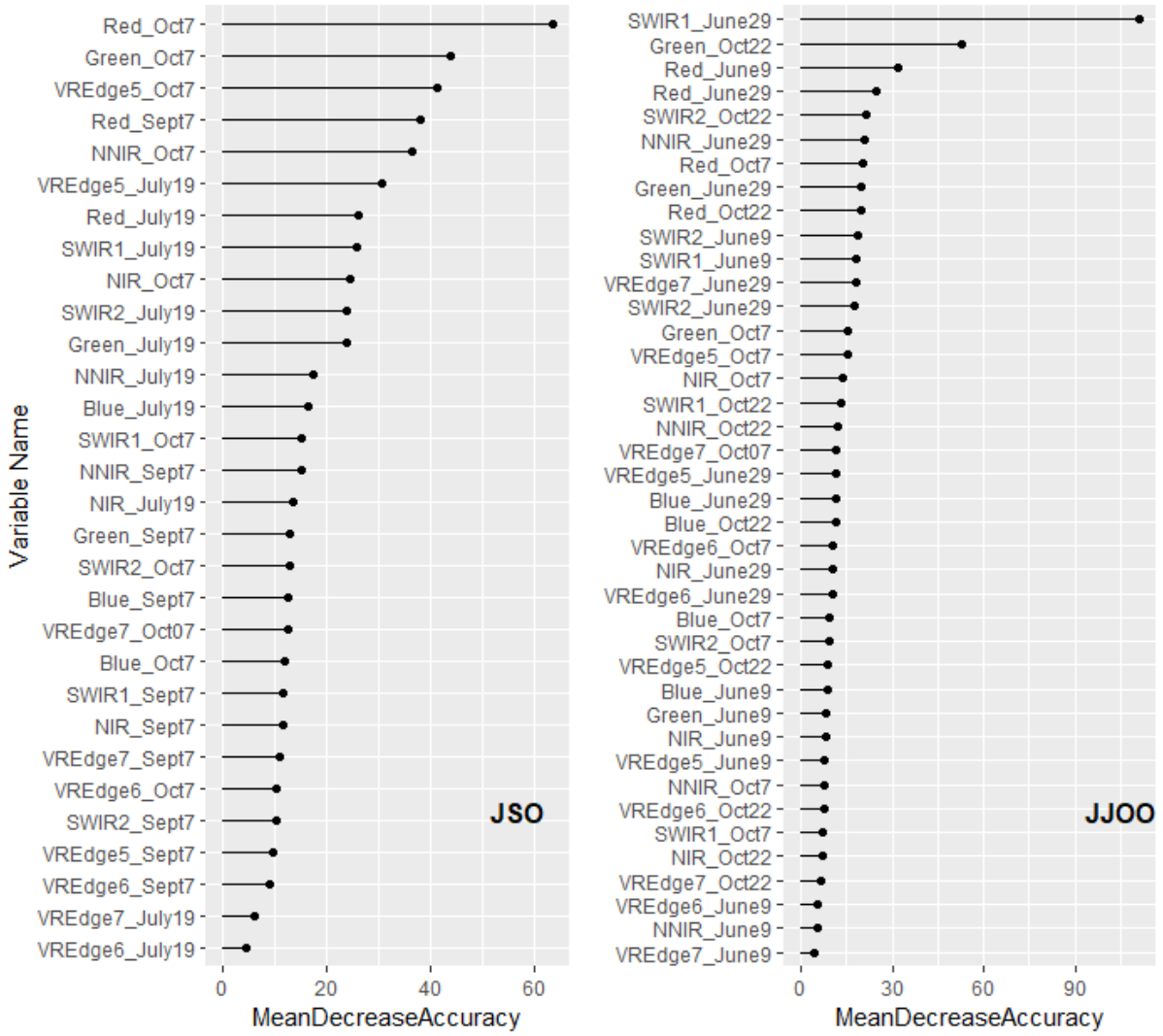


**Figure 3.4:** Variable importance for different combinations of the satellite images according to the variable importance measure from the Random Forest. JSO=July19, Sept7 and Oct22; JJOO=June9 and 29, October7 and 22.

The 2018 image models had a different OOB error compared to 2017. We can see the importance of the October data in the 2018 models. Variable importance within the single date images shows importance with the Red, Green, SWIR and the vegetation red edge bands. Interestingly the Blue band becomes important in the September 27 model, while the NIR bands stands out as an important variable on the October 22 image.

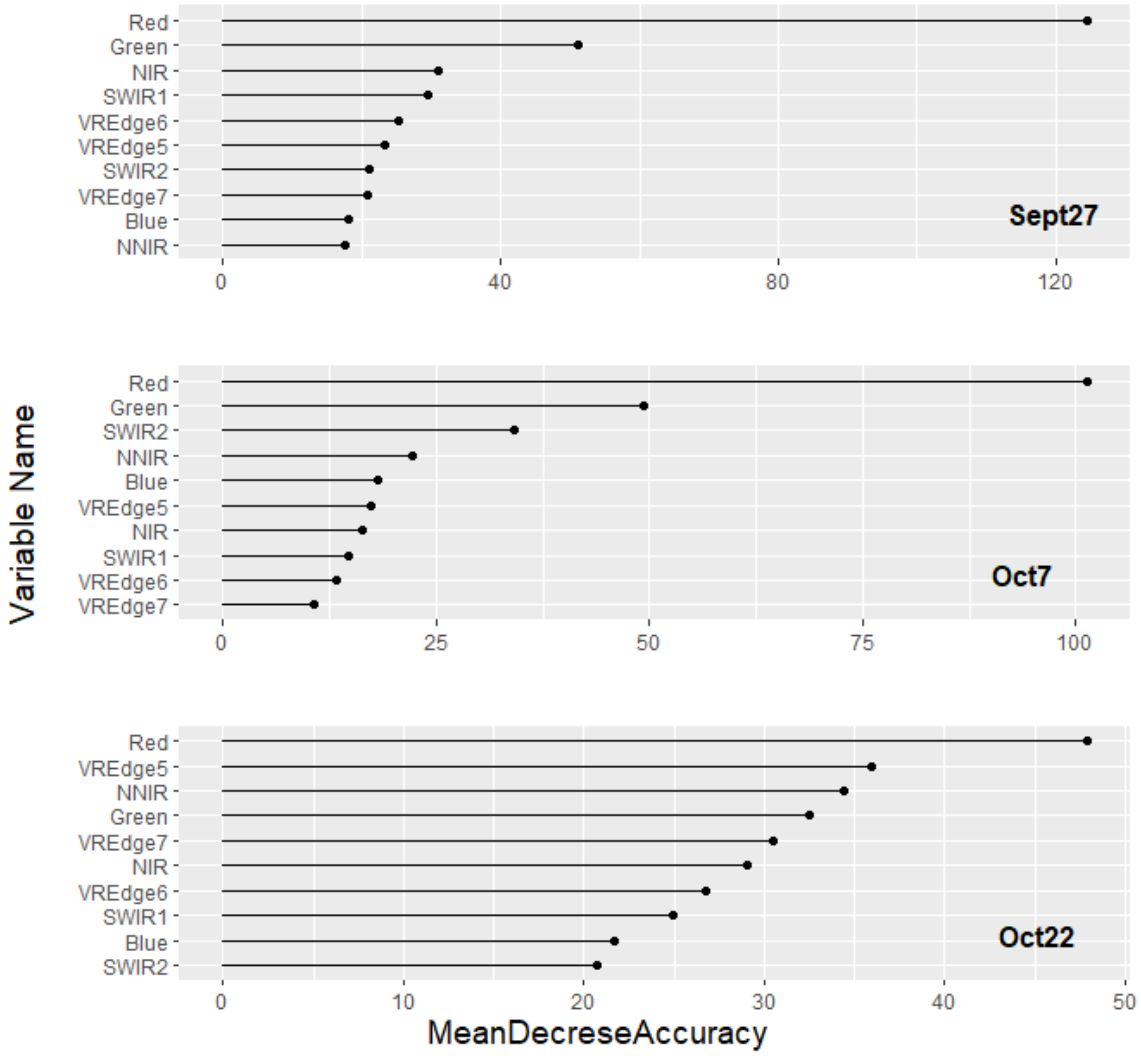


**Figure 3.5:** Variable importance for multi-temporal images. The combinations are SO=September 27 and October22; SOO=September27, October7, October22

In the combination image date models, namely September 27 and October 22 (SO) and Sept27_Oct7_Oct22 (SOO) the variables which are important include the Red band from both September and October. The green band from October 22 also seems relatively important as well. The vegetation red edge and SWIR band from both images also have some importance in the Sept27_Oct22 image date combination model. The Sept27_Oct7_Oct22 image combination might show the same OOB error with the Sept27_Oct22 images combination but with less variable showing importance in the model.

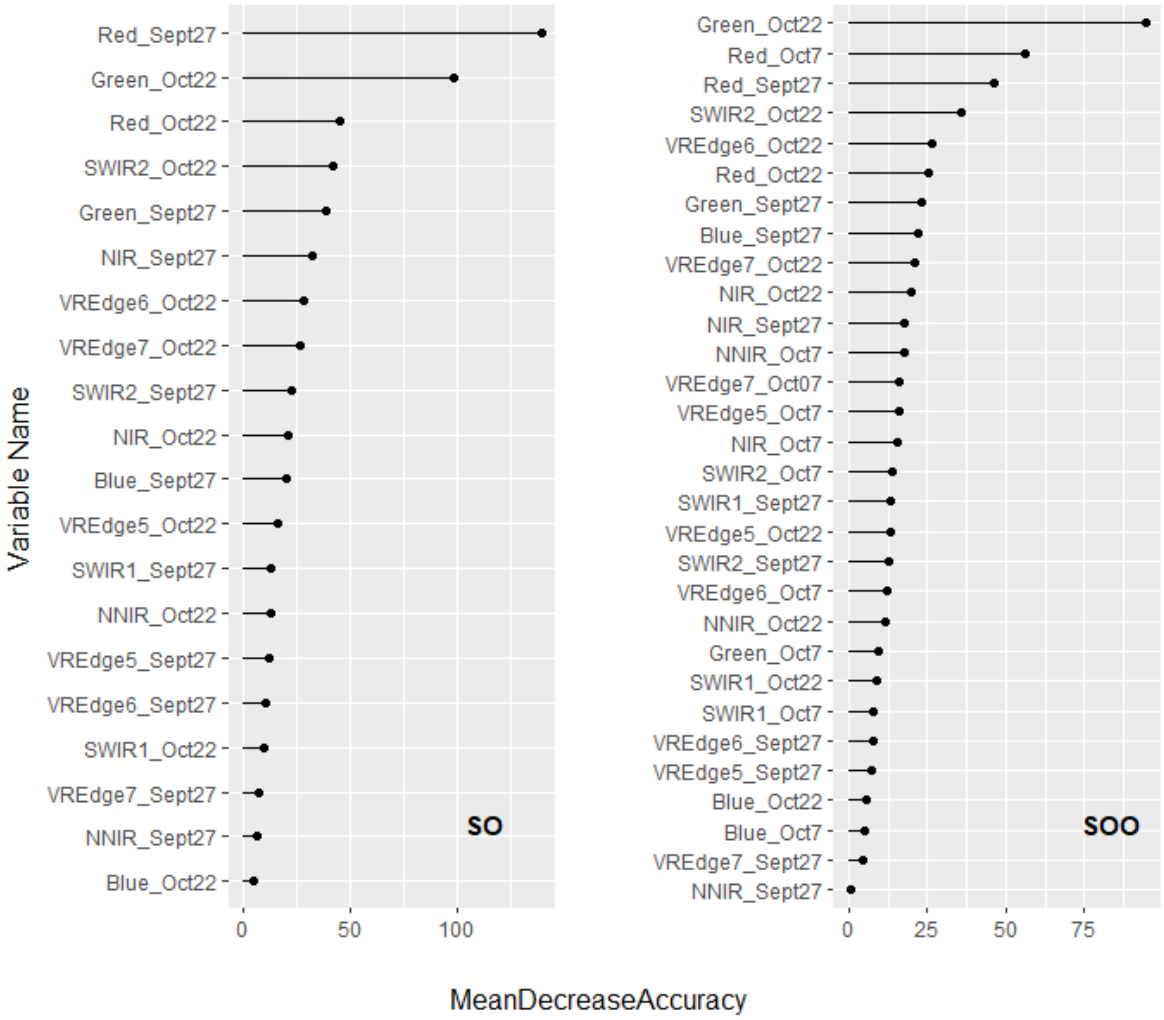


**Figure 3.6:** 2018 Variable importance for single date images out of the best model images.

### 3.1.2 Classification

The October 22 date showed relative importance model performance for both 2017 and 2018. Figure 3.7 shows the Saponé landscape in false color infrared before image classification.

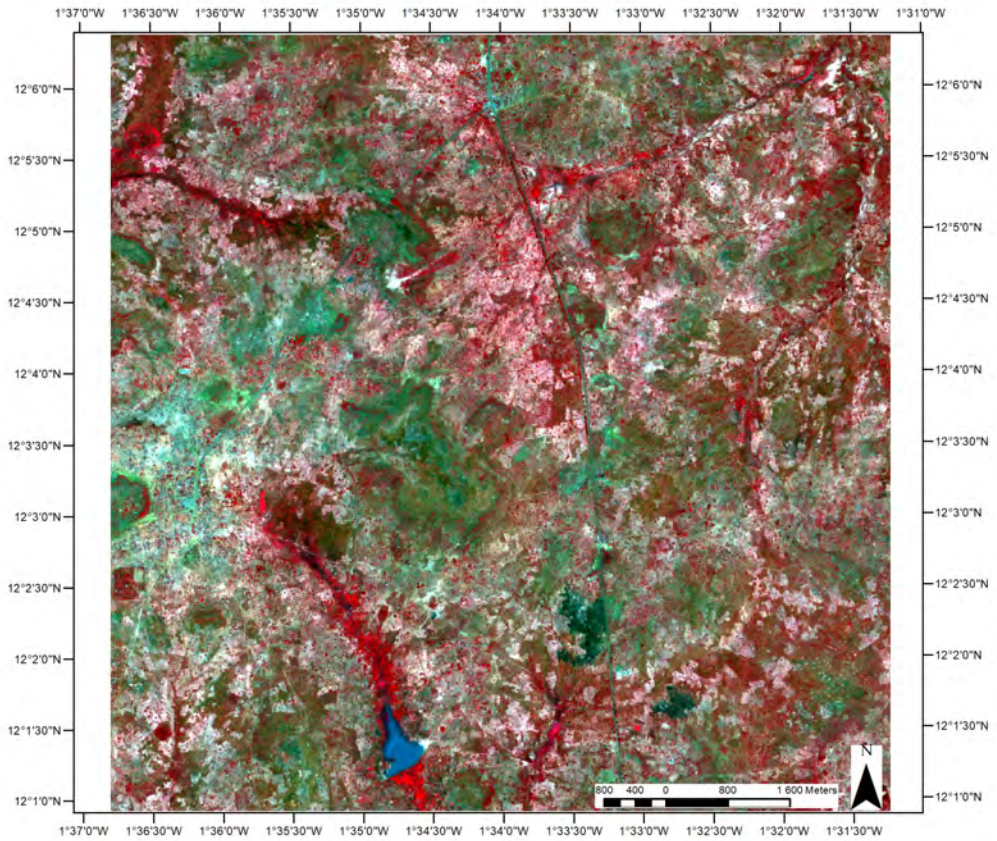


**Figure 3.7:** Sentinel-2 image from 22 October 2017 displayed in false color Infrared over the Saponé landscape.

#### 3.1.2.1 Classification of 2017 and 2018 images

The final classification model is selected based on the parameters from the most accurate model (lowest OOB error). In the case for 2017, the RF model (mtry=30, ntree=2000) using all bands from the October 7 and October 22 2017 images was used. The landcover map is shown in Figure 3.8.

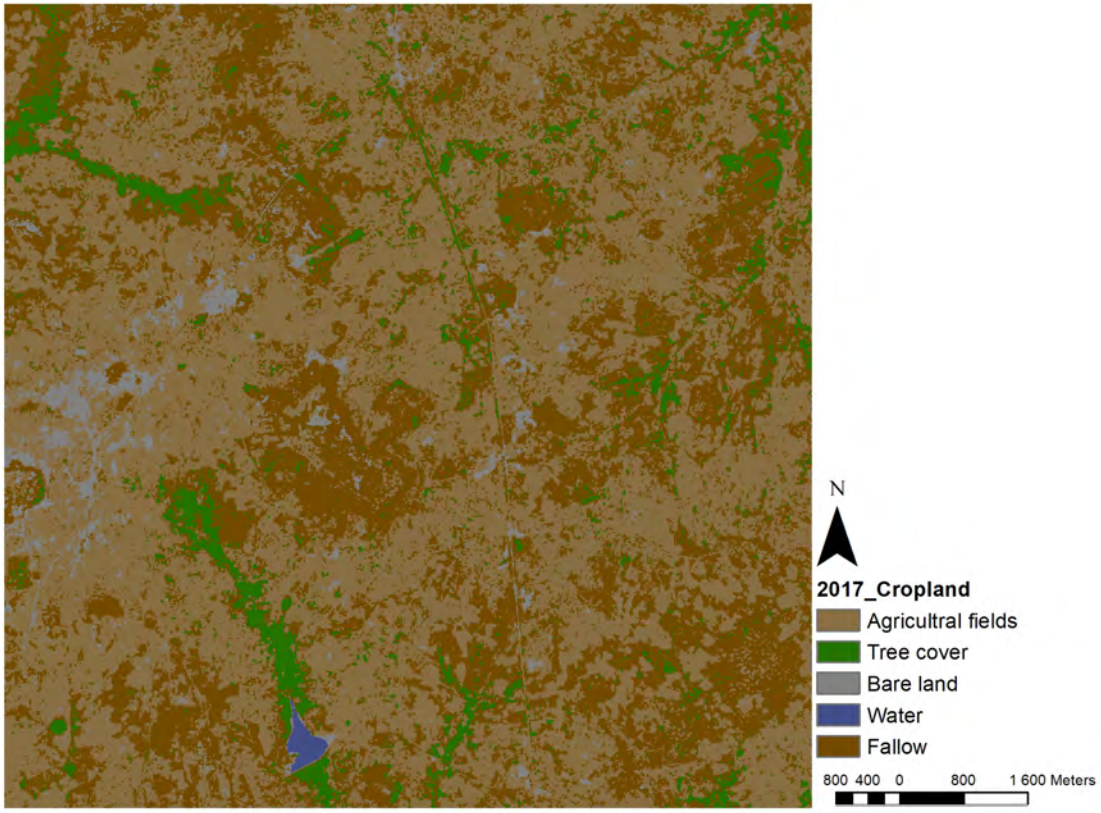


**Figure 3.8:** Land cover classification using the best predictive model from random forest with the October 7 and October 22 2017 images (OO).

For 2018, the RF classifier used only the October 22 image, as multi-temporal imagery for 2018 did not result in a lower OOB error. Figure 3.9 depicts the land cover classification for the 2018 model.

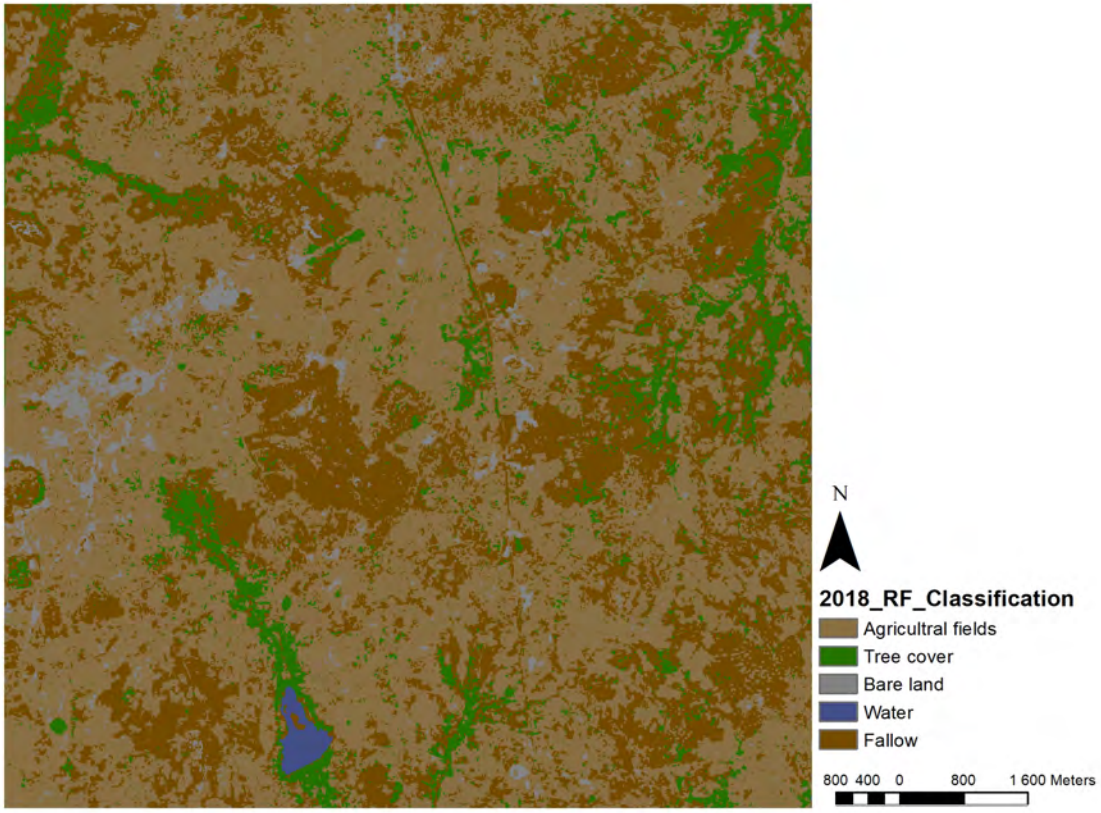


**Figure 3.9:** Land cover classification using the best predictive model from random forest with the single date October 22, 2018 image.

The classification accuracy assessment using cross-validation shows that the OO 2017 model gives an overall accuracy of 94.7%, and a Kappa coefficient of 0.93 (Table 3.1). While, 22 October 2018 model shows an overall accuracy of 90.9%, and a Kappa coefficient of 0.89 (Table 3.2).The confusion matrices provided for the 2017 and 2018 classifications show varying class errors. The producer's and Users's accuracy for Agricultural fields (Agric. Fields) in 2017 show 96%, 93% and 2018 model are 91% and 90% respectively. Agricultural fields were confused with fallow and bare land, while fallow was also confused with tree cover. Looking at the Producers and Users Accuracy on Table 3.1 and 3.2, it is clear the confusion between the agricultural fields, fallow and bare land within the landscape.

**Table 3.1:** Confusion matrix from all bands of October 7 and October 22 2017 (OO) random forest classification with Producer's and User's accuracy (PA, UA) for each class.

| | Agric. fields | Tree cover | Fallow | Water | Bare land | UA(%) |
|---|---|---|---|---|---|---|
| Agric. fields | 51 | 0 | 1 | 0 | 3 | 93 |
| Tree cover | 0 | 31 | 0 | 0 | 1 | 97 |
| Fallow | 1 | 0 | 46 | 0 | 1 | 96 |
| Water | 0 | 0 | 0 | 6 | 0 | 100 |
| Bare land | 1 | 1 | 1 | 0 | 43 | 93 |
| PA(%) | 96 | 97 | 98 | 100 | 88 | **94.7** |

**Table 3.2:** Confusion matrix from 22 October 2018 random forest classification with Producer's and User's accuracy (PA,UA) for each class.

| | Agric. fields | Tree cover | Fallow | Water | Bare land | UA(%) |
|---|---|---|---|---|---|---|
| Agric. fields | 52 | 0 | 2 | 0 | 4 | 90 |
| Tree cover | 0 | 38 | 0 | 0 | 2 | 93 |
| Fallow | 2 | 1 | 47 | 0 | 2 | 91 |
| Water | 0 | 0 | 0 | 6 | 0 | 100 |
| Bare land | 3 | 2 | 0 | 0 | 49 | 91 |
| PA | 91 | 93 | 96 | 100 | 86 | **90.9** |

The Producer's and User's accuracy in each class depict class error variations. Figure 3.10 below shows the spectral signatures of the different Sentinel-2 bands on the best model October images in 2017 and 2018 (OO_2017 and October 22 2018). Spectral responses show the distinct spectral signatures for water, while fallow and agricultural fields, show a similar pattern.

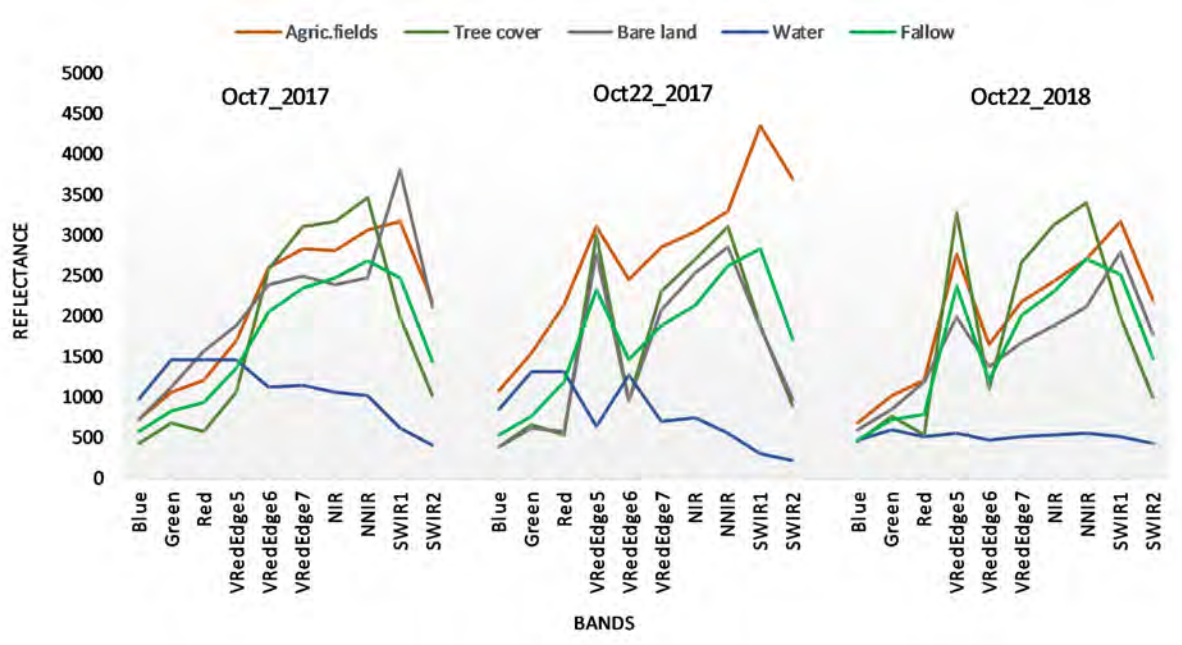


**Figure 3.10:** Mean spectral signatures of five land cover classes of interest at the study area from Sentinel-2 October imagery in 2017 and 2018.

### 3.1.3 Cropland Mask

The land cover classification results for 2017 and 2018 having the best overall classification accuracy were used to create cropland masks for each year. Figures 3.11 and 3.13. The cropland mask for 2017 had 57.3% of cropland area while for 2018 it was 40.8%.

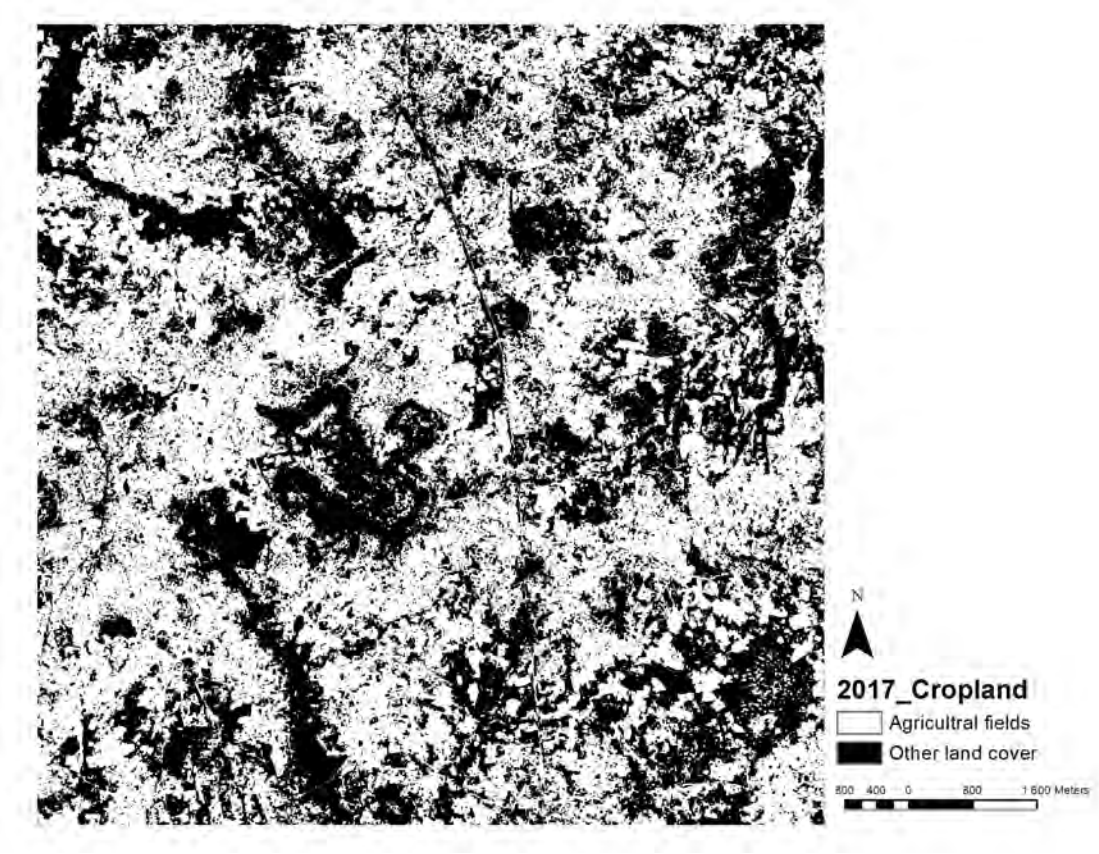


**Figure 3.11:** Cropland mask from random forest classification with best model from 2017, OO_2017. White areas represent cropland area.

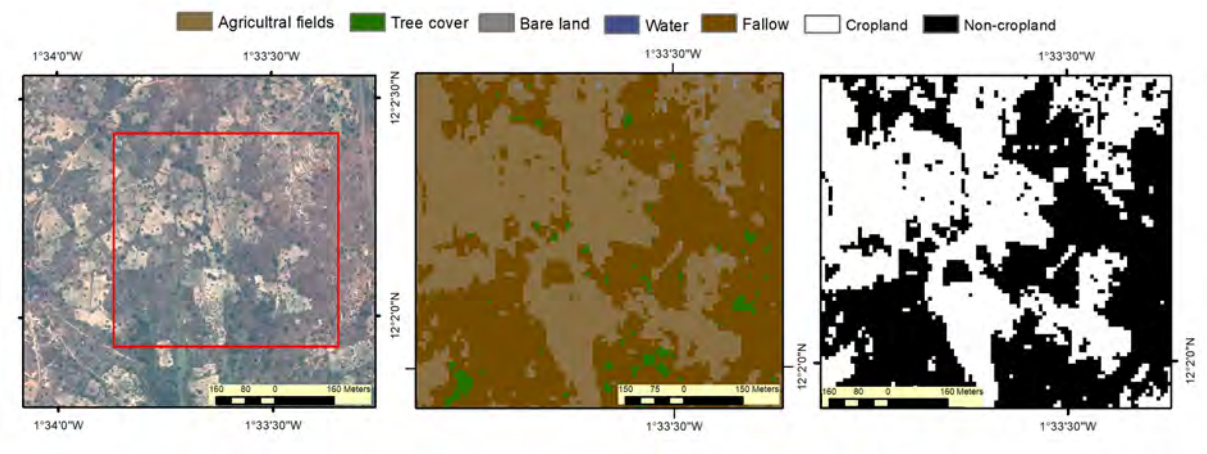


**Figure 3.12:** Visual close up on 2017 products, from left to right; Pléiades image, land cover classification and cropland mask.

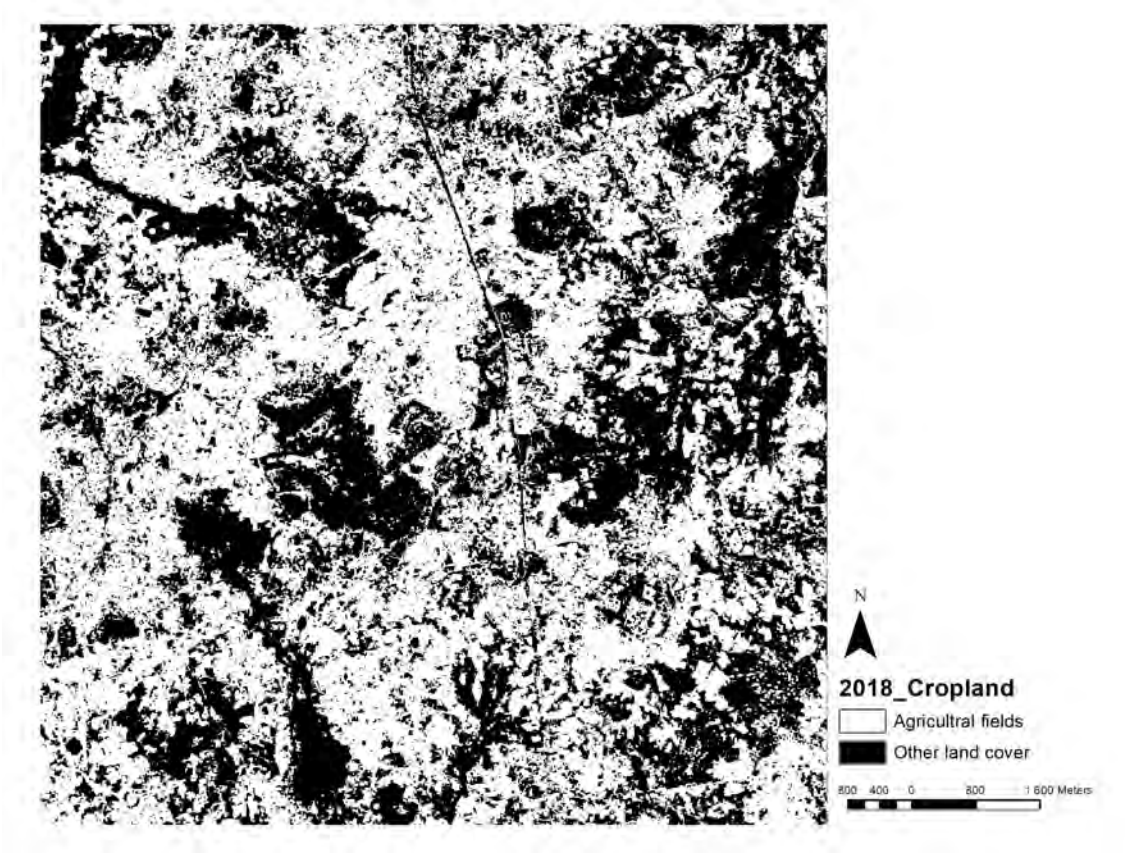


**Figure 3.13:** Cropland mask from random forest classification with best model. White areas represent the cropland area in 2018.

The accuracy of the 2017 cropland mask is much lower at OA= 0.70, than the classification results. While producer's and user's accuracy for the cropland and non-cropland class is presented in Table 3.3.

**Table 3.3:** Confusion matrix between Cropland mask and Pléiades image with randomly sampled points.

| | Cropland | non-Cropland | Total | UA(%) |
|---|---|---|---|---|
| Cropland | 54 | 17 | 71 | 76 |
| non-Cropland | 16 | 25 | 41 | 39 |
| Total | 70 | 42 | 112 | |
| PA(%) | 77 | 40 | | **OA = 70.5%** |

In Figure 3.11 (2017) and 3.13 (2018), the cropland mask is overlaid on the high-resolution Pléiades images obtained for this study. The black represents the other land cover, while the visible part of the Pléiades image is the cropland area within the landscape. There are differences compared to the 2017 cropland mask.

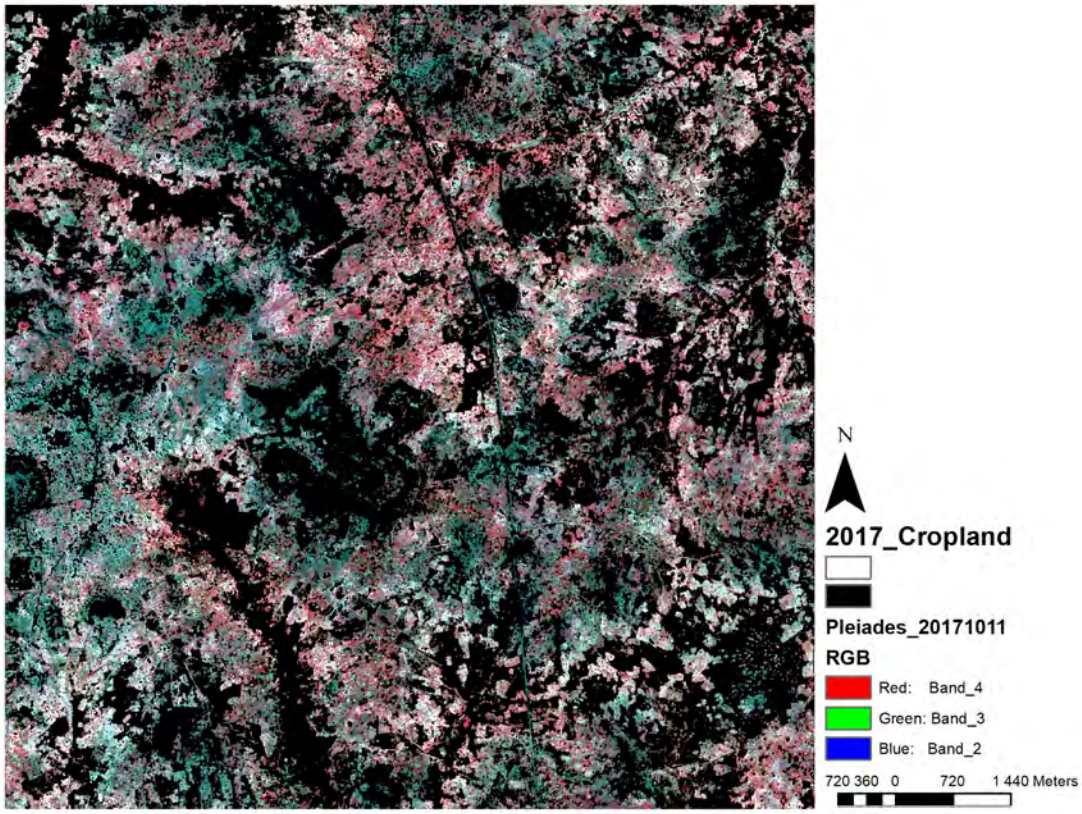


**Figure 3.14:** Cropland mask/Agricultural field land cover overlaid on Pléiades (0.5 m) image for visualisation of the cropland area.

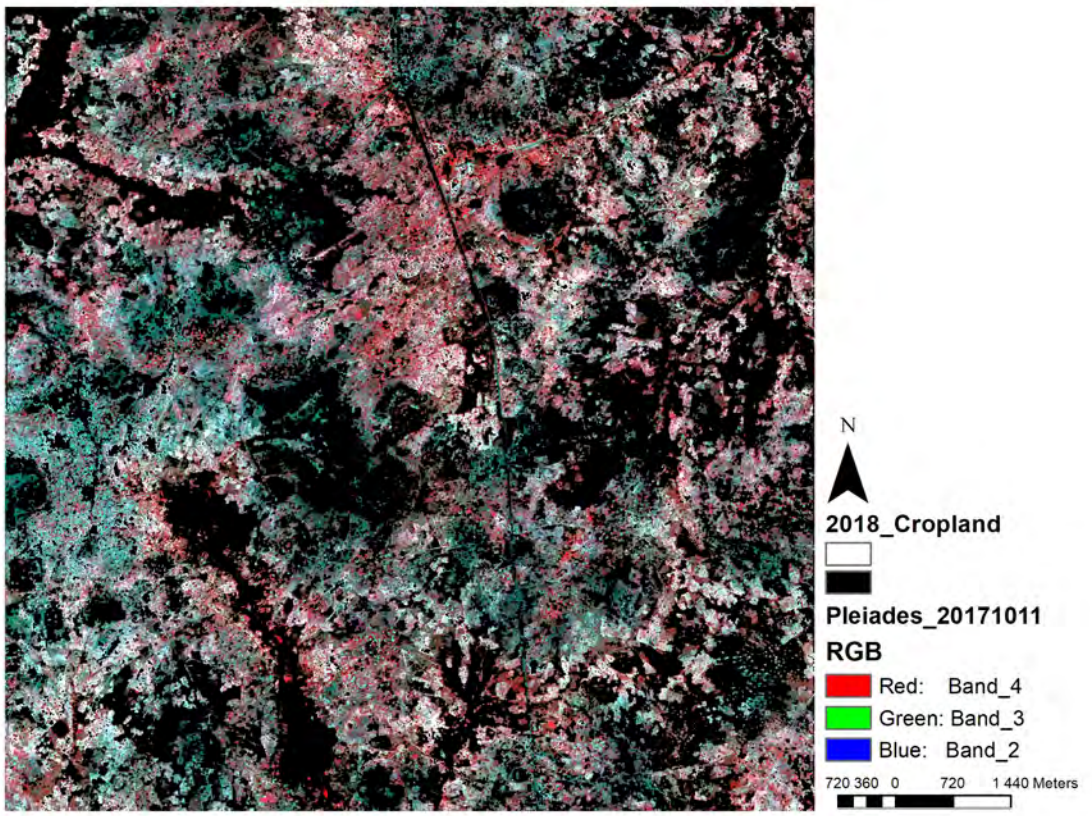


**Figure 3.15:** Cropland mask/Agricultural field land cover overlaid on NIR,R,G Pléiades (0.5 m) image for visualisation of the cropland area.

## 3.2 Tree Cover estimation

### 3.2.1 Variable Importance

Figure 3.16 depicts the variable importance based on the percent Mean Squared Error (MSE) from the random forest regression algorithm, different from the RF classifier. The vegetation index NDVI showed importance in the October 22 model tested. The June image NDVI is not as important as the Green, vegetation red edge and SWIR bands for the June model it ranks lowest with the other vegetation index SR. The SR vegetation index ranks low in percent MSE for both June 29 and October 22 model. The vegetation red edge bands in both June and October models show high importance in %MSE.

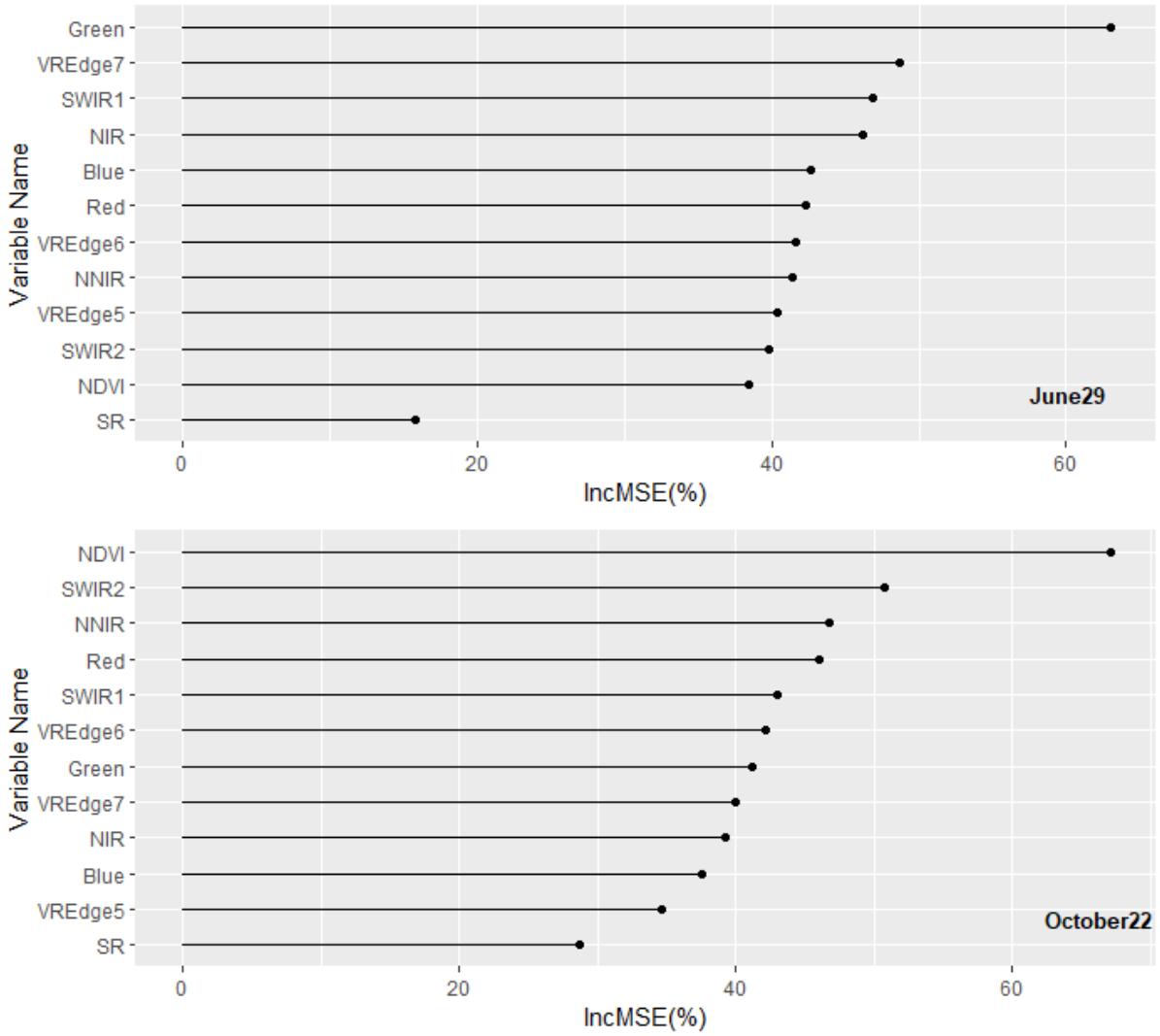


**Figure 3.16:** Predictor variable importance for the tree cover estimation models using a single date 2017 June 29 and single date October 22 image.

The bands ranked differently when in a multi-temporal model (June 29 and October 22 2017). Figure 3.17 presents the importance of the October 22 NDVI variable. The highest ranked bands are from the October 22 image. The June 29 NIR band ranks fourth, surpassing the October 22 red-edge bands.

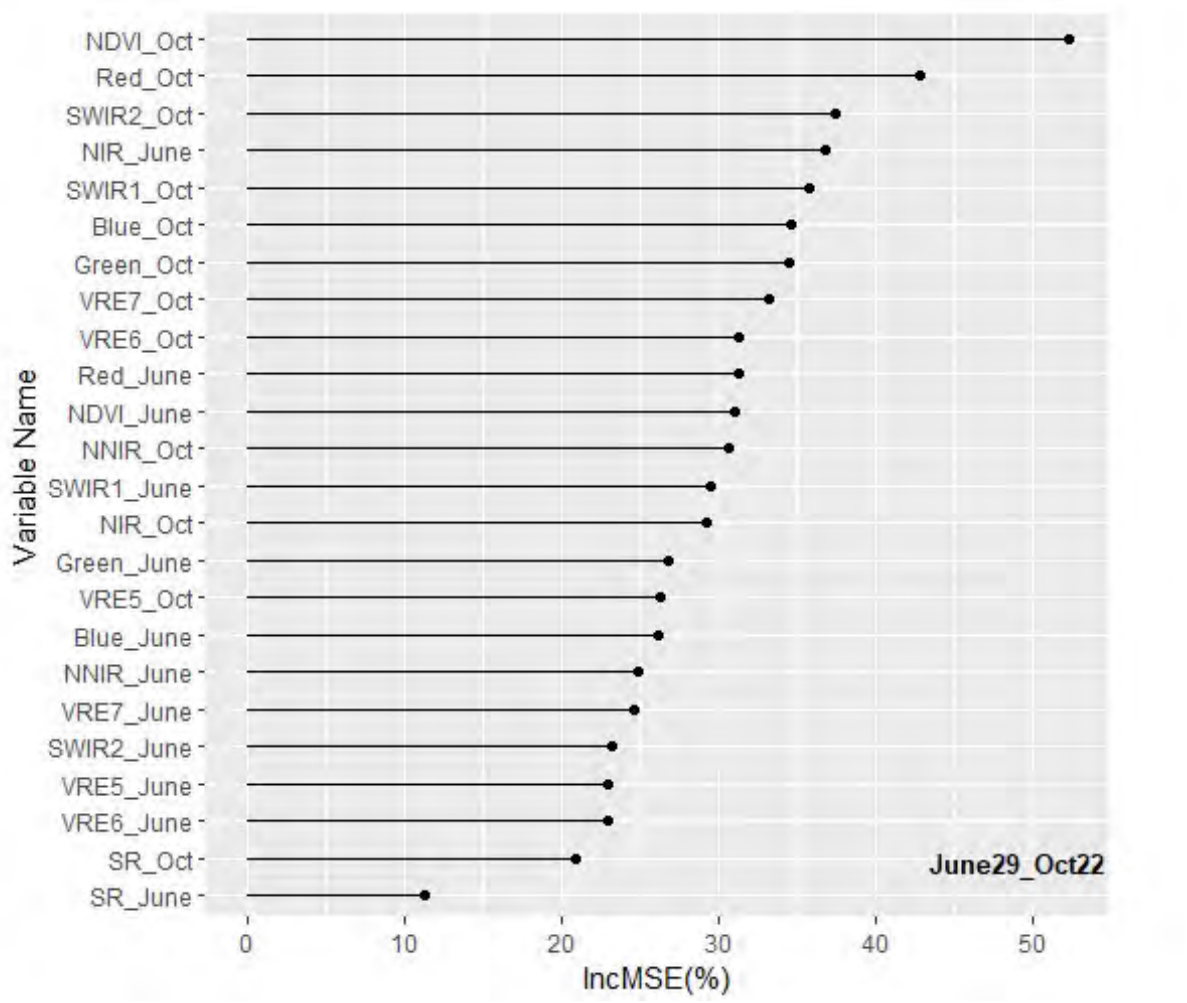


**Figure 3.17:** Predictor variable importance for the tree cover estimation using multi-temporal June 29 and October 22 images model.

Percent of variance explained ($R^2$) and Root mean Squared Error (RMSE) was used to evaluate the regression performance. The images tested for single date models, June 29 and October 22, 2017 had the lowest OOB error with 13.9% and 8.56%, respectively. Predictive abilities of the single date images were less significant than the multi-temporal predictive abilities, where the combination of July and October images provided the better model with percent variance explained of 41.6% (Table 3.4). Bands used in the models were selected according to the variable importance cross selected with varselRF. The variable importance for regression selected the best bands for the model prediction. The selected variables to fit for the multi-temporal model were 12 out of 24. Namely: (i) Blue - October 22 (ii) SWIR2 - June29 and October22 (iii) Green - June29 and October22 (iv) Red - October22 (v) NIR - October22 (vi) VREdge6 - October22 (vii) VREdge7 - October22 (viii) NNIR - October22 (ix) SWIR1 - June29 (x) NDVI - October22.

**Table 3.4:** Results of Random Forest regression model performance for tree cover estimation.

| | mtry | % variance explained | RMSE | MSR |
|---|---|---|---|---|
| June 29 | 2 | 0.21 | 23.54 | 294.5 |
| October 22 | 3 | 0.39 | 24.88 | 228.7 |
| June29 and October22 | 6 | 0.42 | 24.89 | 218.8 |

### 3.2.2 Predicted Tree Cover

The three different models when used to predict tree crown cover resulted in different $R^2$ values. The June_October model produces a slightly higher tree estimate with a 0.92 $R^2$. Table 3.5 presents the regression equation for the tree crown cover estimates using the tree crown observed and tree crown predicted.

**Table 3.5:** Relationship of tree crown cover observed and predicted for the tree cover prediction models. RSE-Residual standard error.

| | $R^2$ | RSE | Regression Equation |
|---|---|---|---|
| June 29 | 0.89 | 4.13 | ∼9.04+0.63x |
| October 22 | 0.91 | 4.35 | ∼6.66+0.73x |
| June29 and October22 | 0.92 | 4.19 | ∼6.43+0.74x |

The best RF model was applied to the raster data, resulting in a full coverage map (Figure 3.18). The predicted tree crown cover ranges from 0.52% to 84.6%, while the observed tree crown cover ranges from 0% to 100%. A scatter plot depicting the observed tree crown cover against the predicted tree crown cover is in presented in Figure 3.19. The predicted tree crown cover agrees well to a certain degree with the observed tree crown cover with $R^2$ value equal to 0.92.

The best fit regression model resulted from parameters used of ntree= 2000, mtry (number of variables tried at each split)= 6. This resulted in a Mean of squared residuals(MSR)= 219 and percentage of variance explained= 42%. The cross-validated regression model resulted in median permuted percent variance explained= 39.51% and cross-validation RMSE= 15.1. The results were also assessed visually in comparison to the Pléiades image, and the results appear reasonable. The significance of the multi-temporal image is visible in the predicted tree crown cover map produced from the random forest regression.

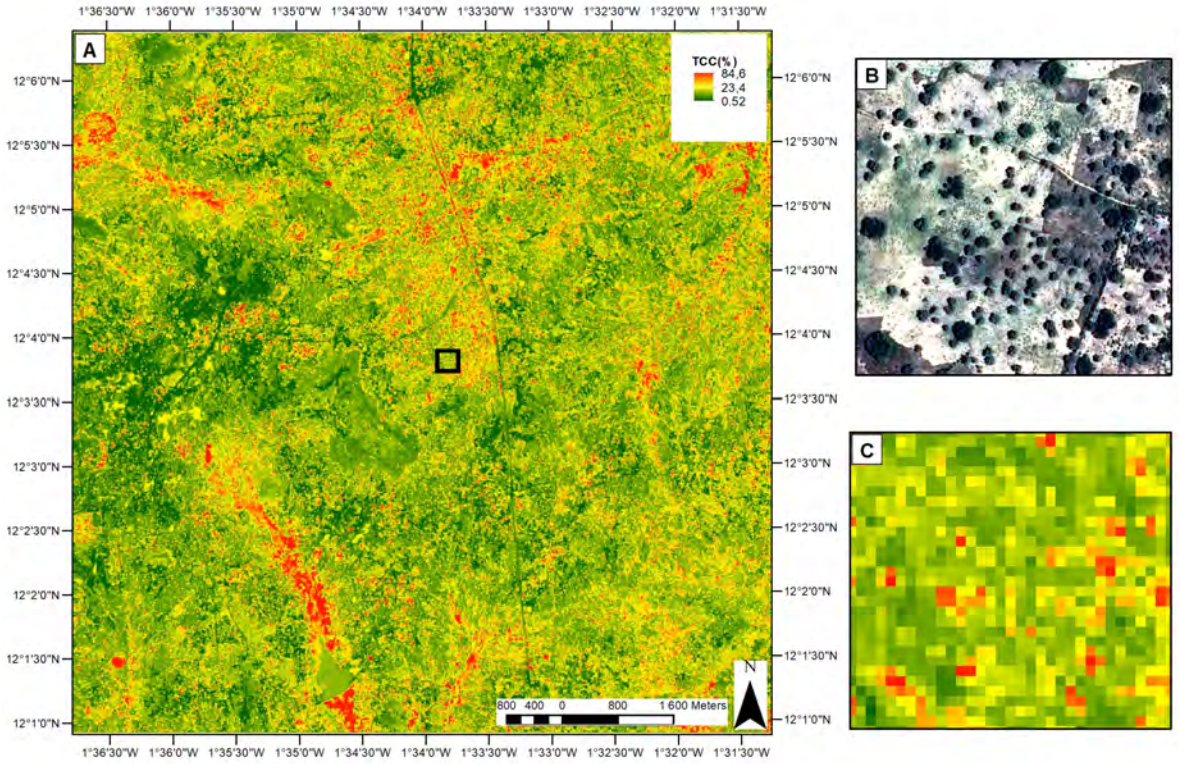


**Figure 3.18:** Percent tree cover result map. A)percent tree cover within Saponé landscape with more detailed area (black square) shown in B and C, where B) shows Pléiades data in true color with trees visible in cropland landscape, and C) Percent tree cover result.

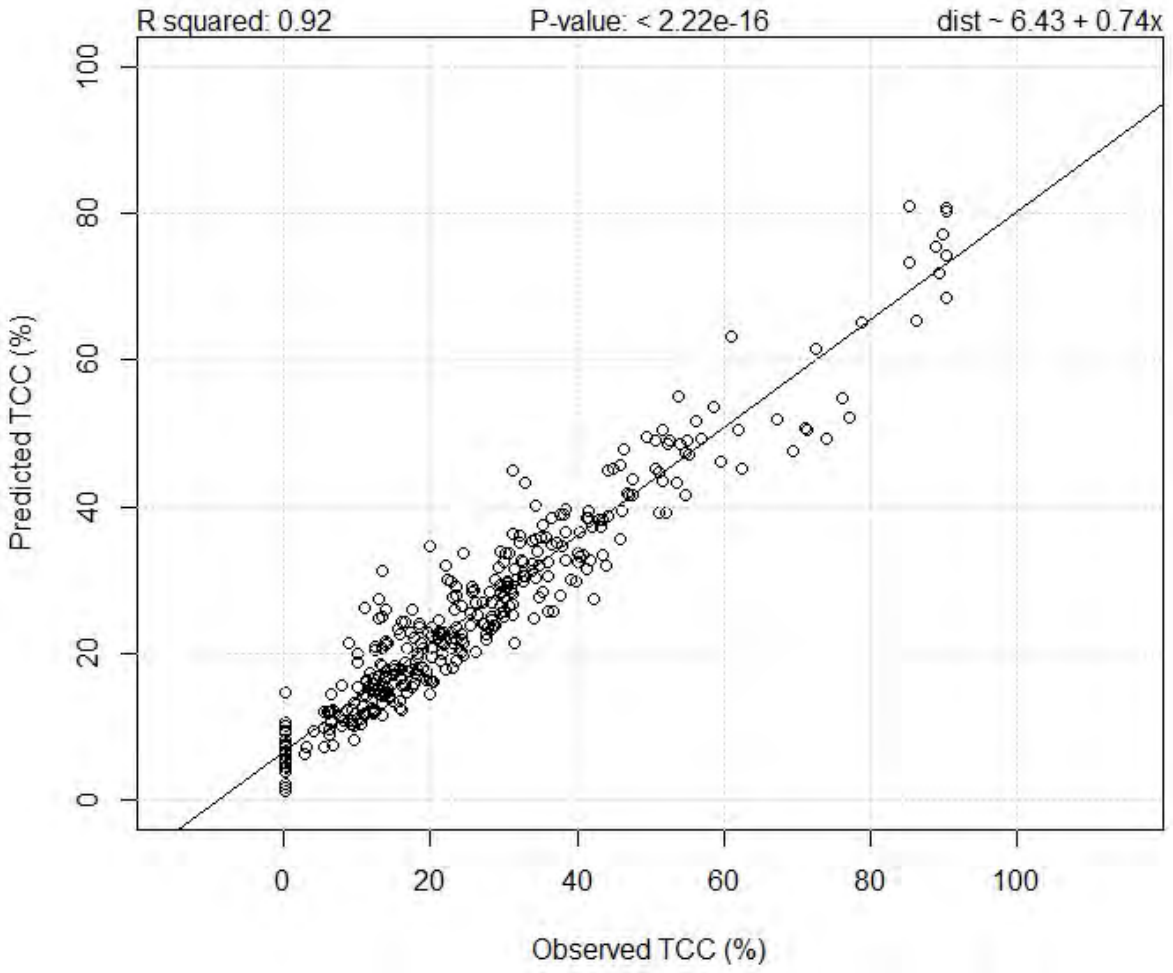


**Figure 3.19:** Relationship between observed and predicted tree canopy cover using the combined June and October (multi-temporal images) model.

# 4
# Discussion

The discussion of the results begin with the land cover classification, exploring the relationship Sentinel-2 bands have with acquisition date of images, highlighting the importance of the different bands for classification with the present and previous studies. Further, I discuss the role Sentinel-2 bands can take in making estimates for tree cover in the Saponé parkland landscape of Burkina Faso. Finally, the different approaches taken in the study and implications to the accuracy of the results are discussed. The results show that discrepancies exist and will be discussed. Implications of the results and future research directions are also presented.

## 4.1 Land cover classification and cropland mask

The cropland mask visually shows an accurate mask with agricultural fields. Although the end goal of most cropland masks is for use in estimating yields for food security purposes within a region and country (Defourny et al., 2019). The ability to identify agricultural fields in satellite imagery is becoming more and more important in managing and monitoring landscapes. It is also interesting to observe that landscape heterogeneity might become a major factor in choice of acquisition dates, when knowledge of vegetation senescence is best for estimating tree cover versus land cover when classifying the landscape with remote sensing. Diversity of spectral properties for croplands especially the inclusion of fallow within the landscape is also mentioned in (Xiong et al., 2017). Xiong et al., 2017 also mentions that being able to discriminate between cropland and seasonal grasses within the landscape is important. The result from this study agree, where the confusion of fallow and cropland is clearly seen in Table 3.1 and 3.2.

A more striking suggestion by Jain et al., 2019 from a fairly commercial study finds that the use of micro-satellite (commercial and costly imagery) data to map smallholder yields detecting the most important active fields for yield calculation and making agricultural

interventions using satellite imagery can be achieved at 'low-cost' with quantified yield gain. Meaning the results (quantified yield estimates) of the approach outweighs the initial investment on the combined imagery costs. At the same time, Jain et al., 2019 also reiterates the use efficiency of satellite imagery in comparison to traditional landscape productivity methods of manually measuring yields, and nitrogen, etc. In a broader perspective, Xiong et al., 2017 created a cropland extent map at 30 m spatial resolution using Sentinel-2 and Landsat-8, for the whole African continent. In addition, cropland definition with the 0.25 ha size proves to be limiting for the Saponé landscape, the resulting cropland mask depicts how small field sizes were not able to be masked due to having either tree pixels or fallow. This spectral mixing at 10 m spatial resolution pixels can sometimes be problem (Weinmann & Weidner, 2018), similar to this current study. This result suggests that object-based classifications might have an advantage in this regard. Amini et al., 2018 reports on object-based classification being an option for LULC classifications, with the right segmentation measures taken for each class.

The best land cover classification came from combining the two October 2017 images. Individually, these images already had a low OOB error. This is due to vegetation detail reaching peak senescence during this time (end of wet season) and spectral response is heightened. This reflects the findings of a study in southern Burkina Faso by Liu et al., 2016, which concluded that cropland was not showing well enough (NDVI values) in a wet season image compared to a dry season image with less vegetation. Although, the Liu et al., 2016 study results in single image classifications for the dry season image (November) performing better than the rainy season image (June). It is worth mentioning that this study did not use a multi-year cropland mask because from the initial results of image OOB error assessment, the landscape discrepancies in 2017 and 2018 were apparent enough to affect the multi-year classification and in turn cropland mask results.

The final model with the lowest OOB error used in 2018 was the single-date image for October 22 which had the same model accuracy as the multi-temporal image combinations. This is an example of multi-temporal images sometimes producing more noise rather than increasing the overall accuracy of the classification. This is also shown by the 2017 classification, where the JJOO (June and October images) had 1.56% more error than the JOO. Also, the OO image shows less error than the JOO, while in JOO, the June 29 image variables had more contribution for class discrimination. Additional images can cause noise due to temporal disagreement Matton et al., 2015 and class errors, especially with detailed vegetation reaching peak senescence. Thus, strategic timely acquisition of images is also important and not just the multi-temporally. Liu et al., 2016 show in their study the importance of seasonal features over single date rainy or dry season images.

Although using Landsat time series they suggest integration with Sentinel-2, the study is conducted in a similar landscape in southern Burkina Faso and the results of the current study are consistent with Liu et al., 2016.

The choice of dates and the model performance of the different dates highlights the relevance of image dates choices in accordance with the vegetation cycles (Immitzer et al., 2016). We can see in the OOB error of the images where one of the 2018 September image gives a 13.3% OOB error while the other gives a 28.6% OOB error. The one with less OOB error we can see the cloud effects, thus the differences in these images is due to the weather conditions. Since we have established the importance of the October image, we can interestingly see the latest September image behaving like the October images. Multi-temporal models are evidently beneficial for land cover classifications and tree cover estimations.

The influence of training data samples and their influence on the model is apparent in this study results. The bias that can be introduced by training samples is strong especially within the random forest algorithm (Reese et al., 2014). This study decided not to have the same amount of training samples for water because of the distinct spectral character of water within the landscape. Although, distribution and the number of samples is important in building a model. However, over representation of classes was kept at a minimum with the rest of the classes using the same amount of training samples. Due to the nature of the landscape and agricultural practices, these five major land cover classes are prone to misclassification. Mixed fields, trees, and big changes in fields occur from one year to the next. Mapping of agricultural fields will provide much more information on cropland area within the Saponé landscape.

### 4.1.1 Variable Importance

The overall variable importance measures highlighted the SWIR, Vegetation red edge, green and red bands as important bands for the models. The finding of the present study suggests that different Sentinel-2 bands as variables have different importance for model building in different single and multi-temporal image dates. The findings suggest that the red spectral channels are important for model building in both the regression and classification models. This finding provides evidence that Immitzer et al., 2016 and Valero et al., 2016 have mentioned on the suitability of the Red and SWIR spectral bands in agricultural mapping of agricultural areas more specifically cropland. Further, the 10 m NIR is surpassed in importance by the resampled 20 m bands SWIR and the vegetation red edge bands. For instance some remarks about the spectral channel for B8 (NIR, 10

m) include how it is much wider than B8A (NIR, 20 m) with less characteristic nature, therefore the ability to use it for classification diminishes, which is similar to Immitzer et al., 2016 with results on both the Sentinel-2 NIR bands ranking low in importance for classification of crop type and tree species.

The more surprising correlation is with the Blue bands in the 2018 classification model showing importance. Similar to Liu et al., 2016 who mentions that the Blue band is an important variable within their model at the same time re-iterating greater importance of the SWIR and vegetation red edge bands over the NIR in Savannah ecosystems (a similar variation of agroforestry parkland definition of landscape type that includes scattered woody vegetation and grassland). The Red Edge and Short Wave Infrared bands are highly important variables for vegetation monitoring (Frampton et al., 2013), and most previous studies have used the SWIR and RedEdge bands for agriculturally related vegetation studies Matton et al., 2015, at the same time highlighting the limitations of the bands spatial resolution at 20 m.

## 4.2 Tree cover estimation

The $R^2$ value of 0.42 shows that the relationship between the Sentinel-2 data and the tree crown coverage as measured in high-resolution images was imperfect and cannot be used to estimate tree crown cover. However, it could be used to identify trees rather than estimate tree crown cover percentage over the larger Sentinel-2 data area. From the results in Figure 3.19 it is apparent that the model overestimated 0% tree crown cover, and under-estimated 100% tree crown cover. Figure 3.18 clearly shows how the individual tree crown can be seen in the prediction map with the red pixels. However, there is also tree crown cover where there are no trees.

One assumption on the use of spectral data for tree crown cover percentage is that tree crowns have higher values in the red, green and near-infrared bands, while the surrounding area has lower values (Yang et al., 2019). Thus, tree crown percentage within a woodland and parkland ecosystems can be detected due to mature individual trees within the landscape, unlike plantations and forested areas. Interestingly, Brandt et al., 2016 reports on woody vegetation still having prominent NDVI values even after the rainy season compared to herbaceous vegetation, thus, explains the importance of vegetation phenology. Bolyn et al., 2018 suggests the use of high spatial resolution data in combination with Sentinel-2 for a better spatial precision combined with the discrimination power of Sentinel-2 spectral data. In relation to this study, obtaining reference data from the

strategically acquired 11 October 2017 (end of wet season), 0.5 m spatial resolution Pléiades image greatly contributed to the agreement of the predicted and observed tree crown cover ($R^2$=0.92) even though the variance explained from the random forest regression was very poor. This was an interesting result as a poor variance will normally result in poor predicted values. FAOSTAT reports 20790 $km^2$ for tree covered area in Burkina Faso from the Climate Change Initiative (CCI) annual land cover maps, in relation to 2480 $km^2$ of woody crops (these are separated from herbaceous crops which are related to the current studies cropland area). This study did not separate the tree cover in this way, but acknowledges the extent different tree species have for detection in satellite imagery and landscape interactions, as mentioned in studies in this area (Karlson et al., 2014; Karlson and Ostwald, 2016).

In a similar study on the same landscape, Karlson et al., 2015 mapped tree canopy cover using five predictor variables from a Landsat-8 image and supplemented field data with World View-2 imagery, achieving a 0.77 $R^2$. The Karlson et al., 2015 study also tests use of multi-temporal imagery from dry season imagery October 2013 to March, 2014. In this regard, the present study using Sentinel-2 data achieves a poor result for tree cover estimation, achieving a 0.42 $R^2$. This shows how the heterogeneous nature of the Burkina Faso landscape can be complicated for the mapping of the landscape with the different seasons and sensors. Similarity of this study and Karlson et al., 2015 though is the importance of the vegetation red edge bands, highlighting spectral separation of parkland tree species due to leaf pigment content. Regarding limitations, the RF regression trees rely extensively on the data range of training data provided, and do not extrapolate beyond the input data values. It is possible that a linear regression may be a more effective method to estimate tree crown cover.

Percentage increase in mean square error (%IncMSE) for the tree crown cover estimation variable importance, highly rank NDVI, SWIR and surprisingly NNIR Sentinel-2 bands. Furthermore, the spectral indices used for tree cover estimation (SR, NDVI), showed that NDVI was more important for the models, yet showing varying importance in all models. When combined in the multi-temporal model, the October 22 NDVI was the most important variable for the model. The October model as the best model, shows a limited number of variables being selected as important. One red edge band, SWIR, Green and Red band are the only bands highlighted as important. Therefore, the importance of the NDVI is similar to previous studies using vegetation indices for tree cover estimations (Karlson et al., 2015; Yang et al., 2019). Additionally, the importance of the NDVI might be influenced by the calculation from the original Sentinel-2 10 m spatial resolution bands (Red and NIR).

## 4.3 Relevance for the Saponé landscape

The production of crop masks and tree cover estimation was part of a larger research project which will analyze geospatial data on tree cover and crop production to uncover the role of trees in the agroforestry landscape of Burkina Faso. It is important that free satellite data, such as Sentinel-2, are of sufficient quality to provide this information. This study looks at an area of 10x10km landscape whereby the total land area of Burkina Faso is 273,600 $km^2$ with 61,000 $km^2$ of cropland area and monitoring of these cropland areas is of paramount importance.

Interestingly, a study by Félix et al., 2018, which is unrelated to use of satellite imagery, gives insight in future project work which will involve productivity of the landscape. The Félix et al., 2018 study concludes on improved soil carbon, millet and sorghum yields in parklands with shrubs and trees as we see in the Saponé landscape of this study. Our findings revealed that cropland masks at 10 m over most of the countries in West Africa within the SSZ are a new thing. For instance, Defourny et al., 2019 states only in 2016, Mali had the first 10 m cropland mask product delivered. While, Defourny et al., 2019 explores how the Sen2-Agri tool developed for cropland monitoring by the European Space Agency can be beneficial for national monitoring and enhancing national agricultural statistics.

Importantly, Defourny et al., 2019 mentions that the system will definitely have glitches in agricultural areas frequently covered by clouds and with mixed cropping system, which is highly relevant for the current study area limitations in Burkina Faso. However, Sen2-Agri proves the relevance of the 10 m resolution capability of the Sentinel-2 images for high resolution cropland monitoring at national scale. In addition, Forkuor et al., 2018 with several other research papers suggest the complimentary use of Sentinel-2 with Landsat-8 satellite data, considering the temporal resolution that is spanned when using both sensors. Overall, multi-sensor land use and land cover studies have produced more accurate LULC maps (Forkuor et al., 2018; Xiong et al., 2017), and complimentary availability of free images among sensors is also something to explore further.

Finally, the results have shown the power of Sentinel-2 spectral data. Vegetation mapping, especially in the direction of cropland masks, can be achieved using the Sentinel-2 10 m resolution and discrimination power of the 20 m vegetation red edge bands. Therefore, more powerful than not is the open access of such high-resolution imagery for the monitoring of landscapes which are under pressure due to climate change which affects food security and landscape productivity.

# 5
# Conclusion and Future work

This study has explored the capabilities of Sentinel-2 bands in creating a cropland mask and tree cover estimation. Variable importance is explored in Sentinel-2 bands for land classification and tree cover estimation. Two years were set apart to assess the multi-temporal and yearly capabilities, in wet season images (May to October). Data was classified and predicted using the Random Forest algorithm. Field data and Pléiades image were used for training data and accuracy assessment respectively.

This study produced two (2017 and 2018) landscape level cropland masks at 10 m. Accuracy of 2017 cropland mask was 71%. From initial land cover classification which had an overall accuracy of 95% and 91%, respectively. Additionally, Sentinel-2 underestimated tree cover of higher percentage and overestimated sparse tree cover, with the range of predicted tree crown cover from 0.59% to 85.4%.

Main sources of error in this study range from the resampling of the 20m bands, training data to mapping an agroforestry parkland, where inter-cropping and cropping practices are diverse. Based on the robust use of the Random Forest algorithm, we recommend using Sentinel-2 for cropland masks. Based on the results of this study, the Sen2-Agri algorithm might be an extensive and advantageous tool creating landscape level cropland mask as we have done. This will allow for better comparison with global cropland cover maps already existing, with JECAM, CCI_LC and GEOGLAM, which are main sources of reference for cropland mapping globally and within this study. With this, future work can increase tree identification by using a threshold of 70% upwards creating a "tree mask".

Overall this study has shown the capabilities of Sentinel-2 are limited to vegetation monitoring studies that do not need estimation of yield and maybe extensive crop identification especially in heterogeneous landscapes. Further research on the assessment of capabilities of Sentinel-2 in agroforestry parklands can include the assessment of the sizes of agricultural fields.

# Bibliography


Amini, S., Homayouni, S., Safari, A., & Darvishsefat, A. A. (2018). Object-based classification of hyperspectral data using random forest algorithm. *Geo-spatial information science*, *21*(2), 127–138.

Bargués Tobella, A, Reese, H, Almaw, A, Bayala, J, Malmer, A, Laudon, H, & Ilstedt, U. (2014). The effect of trees on preferential flow and soil infiltrability in an agroforestry parkland in semiarid burkina faso. *Water Resources Research*, *50*(4), 3342–3354.

Belgiu, M., & Drăguţ, L. (2016). Random forest in remote sensing: A review of applications and future directions. *ISPRS Journal of Photogrammetry and Remote Sensing*, *114*, 24–31.

Birth, G. S., & McVey, G. R. (1968). Measuring the color of growing turf with a reflectance spectrophotometer 1. *Agronomy Journal*, *60*(6), 640–643.

Bolyn, C., Michez, A., Gaucher, P., Lejeune, P., & Bonnet, S. (2018). Forest mapping and species composition using supervised per pixel classification of sentinel-2 imagery. *Biotechnologie, Agronomie, Société et Environnement*, *22*(3), 16.

Brandt, M., Hiernaux, P., Tagesson, T., Verger, A., Rasmussen, K., Diouf, A. A., Mbow, C., Mougin, E., & Fensholt, R. (2016). Woody plant cover estimation in drylands from earth observation based seasonal metrics. *Remote Sensing of Environment*, *172*, 28–38.

Breiman, L. (1998). Arcing classifier (with discussion and a rejoinder by the author). *The annals of statistics*, *26*(3), 801–849.

Cetin, M, Kavzoglu, T, & Musaoglu, N. (2004). Classification of multi-spectral, multi-temporal and multi-sensor images using principal components analysis and artificial neural networks: Beykoz case, In *Proceedings xxth international society for photogrammetry and remote sensing-congress*.

Defourny, P., Bontemps, S., Bellemans, N., Cara, C., Dedieu, G., Guzzonato, E., Hagolle, O., Inglada, J., Nicola, L., Rabaute, T., Et al. (2019). Near real-time agriculture monitoring at national scale at parcel resolution: Performance assessment of the

sen2-agri automated system in various cropping systems around the world. *Remote sensing of environment*, *221*, 551–568.

Di Gregorio, A. (2005). *Land cover classification system: Classification concepts and user manual: Lccs* (Vol. 2). Food & Agriculture Org.

Diaz-Uriarte, R. (2007). Genesrf and varselrf: A web-based tool and r package for gene selection and classification using random forest. *BMC Bioinformatics*, *8*. https://doi.org/10.1186/1471-2105-8-328

ESA. (2017). *Land cover cci product user guide version 2. technical report.* http://maps.elie.ucl.ac.be/CCI/viewer/download/ESACCI-LC-Ph2-PUGv2_2.0.pdf (accessed: 2020)

ESA. (2019). *Sentinel missions*. https://sentinel.esa.int/web/sentinel/missions/sentinel-2 (accessed: 2019)

Félix, G. F., Clermont-Dauphin, C., Hien, E., Groot, J. C., Penche, A., Barthès, B. G., Manlay, R. J., Tittonell, P., & Cournac, L. (2018). Ramial wood amendments (piliostigma reticulatum) mitigate degradation of tropical soils but do not replenish nutrient exports. *Land Degradation & Development*, *29*(8), 2694–2706.

Foody, G. M., & Mathur, A. (2006). The use of small training sets containing mixed pixels for accurate hard image classification: Training on mixed spectral responses for classification by a svm. *Remote Sensing of Environment*, *103*(2), 179–189.

Forkuor, G., Dimobe, K., Serme, I., & Tondoh, J. E. (2018). Landsat-8 vs. sentinel-2: Examining the added value of sentinel-2's red-edge bands to land-use and land-cover mapping in burkina faso. *GIScience & Remote Sensing*, *55*(3), 331–354.

Frampton, W. J., Dash, J., Watmough, G., & Milton, E. J. (2013). Evaluating the capabilities of sentinel-2 for quantitative estimation of biophysical variables in vegetation. *ISPRS journal of photogrammetry and remote sensing*, *82*, 83–92.

Freeman, E. A., Moisen, G. G., Coulston, J. W., & Wilson, B. T. (2016). Random forests and stochastic gradient boosting for predicting tree canopy cover: Comparing tuning processes and model performance. *Canadian Journal of Forest Research*, *46*(3), 323–339.

Fritz, S., See, L., Bayas, J. C. L., Waldner, F., Jacques, D., Becker-Reshef, I., Whitcraft, A., Baruth, B., Bonifacio, R., Crutchfield, J., Et al. (2019). A comparison of global agricultural monitoring systems and current gaps. *Agricultural systems*, *168*, 258–272.

Fritz, S., See, L., You, L., Justice, C., Becker-Reshef, I., Bydekerke, L., Cumani, R., Defourny, P., Erb, K., Foley, J., Et al. (2013). The need for improved maps of global cropland. *Eos, Transactions American Geophysical Union*, *94*(3), 31–32.

Ilstedt, U., Tobella, A. B., Bazié, H., Bayala, J., Verbeeten, E, Nyberg, G., Sanou, J., Benegas, L., Murdiyarso, D, Laudon, H, Et al. (2016). Intermediate tree cover can maximize groundwater recharge in the seasonally dry tropics. *Scientific reports*, *6*, 21930.

Immitzer, M., Vuolo, F., & Atzberger, C. (2016). First experience with sentinel-2 data for crop and tree species classifications in central europe. *Remote Sensing*, *8*(3), 166.

Jain, M., Rao, P., Srivastava, A. K., Poonia, S., Blesh, J., Azzari, G., McDonald, A. J., Lobell, D. B., Et al. (2019). The impact of agricultural interventions can be doubled by using satellite data. *Nature Sustainability*, *2*(10), 931–934.

Karlson, M., & Ostwald, J. J. o. A. E., Madelene. (2016). Remote sensing of vegetation in the sudano-sahelian zone: A literature review from 1975 to 2014. *Journal of Arid Environments*, *124*, 257–269.

Karlson, M., Ostwald, M., Reese, H., Bazié, H. R., & Tankoano, B. (2016). Assessing the potential of multi-seasonal worldview-2 imagery for mapping west african agroforestry tree species. *International Journal of Applied Earth Observation and Geoinformation*, *50*, 80–88.

Karlson, M., Ostwald, M., Reese, H., Sanou, J., Tankoano, B., & Mattsson, E. (2015). Mapping tree canopy cover and aboveground biomass in sudano-sahelian woodlands using landsat 8 and random forest. *Remote Sensing*, *7*(8), 10017–10041.

Karlson, M., Reese, H., & Ostwald, M. (2014). Tree crown mapping in managed woodlands (parklands) of semi-arid west africa using worldview-2 imagery and geographic object based image analysis. *Sensors*, *14*(12), 22643–22669.

Knauer, K., Gessner, U., Fensholt, R., Forkuor, G., & Kuenzer, C. (2017). Monitoring agricultural expansion in burkina faso over 14 years with 30 m resolution time series: The role of population growth and implications for the environment. *Remote Sensing*, *9*(2), 132.

Lambert, M.-J., Waldner, F., & Defourny, P. (2016). Cropland mapping over sahelian and sudanian agrosystems: A knowledge-based approach using proba-v time series at 100-m. *Remote Sensing*, *8*(3), 232.

Liaw, A., & Wiener, M. (2002). Classification and regression by randomforest. *R News*, *2*(3), 18–22. https://CRAN.R-project.org/doc/Rnews/

Liu, J., Heiskanen, J., Aynekulu, E., Maeda, E. E., & Pellikka, P. K. (2016). Land cover characterization in west sudanian savannas using seasonal features from annual landsat time series. *Remote Sensing*, *8*(5), 365.

Maranz, S. (2009). Tree mortality in the african sahel indicates an anthropogenic ecosystem displaced by climate change. *Journal of Biogeography*, *36*(6), 1181–1193.

Matton, N., Canto, G., Waldner, F., Valero, S., Morin, D., Inglada, J., Arias, M., Bontemps, S., Koetz, B., & Defourny, P. (2015). An automated method for annual cropland mapping along the season for various globally-distributed agrosystems using high spatial and temporal resolution time series. *Remote Sensing*, *7*(10), 13208–13232.

R Core Team. (2017). *R: A language and environment for statistical computing*. R Foundation for Statistical Computing. Vienna, Austria. https://www.R-project.org/

Reese, H., Nyström, M., Nordkvist, K., & Olsson, H. (2014). Combining airborne laser scanning data and optical satellite data for classification of alpine vegetation. *International Journal of Applied Earth Observation and Geoinformation*, *27*, 81–90.

Rokhmatuloh, R, Al-Bilbisi, H, Arihara, K, Kobayashi, T, Nitto, D, Erdene, B, Hirabayashi, K, Javzandulam, T., Lee, S., Migita, E, Et al. (2005). Application of regression tree method for estimating percent tree cover of asia with quickbird images as training data, In *The 11th ceres international symposium on remote sensing, chiba university, chiba, japan*.

Rouse Jr, J., Haas, R., Schell, J., & Deering, D. (1974). Monitoring vegetation systems in the great plains with erts. *NASA special publication*, *351*, 309.

Sekertekin, A., Marangoz, A., & Akcin, H. (2017). Pixel-based classification analysis of land use land cover using sentinel-2 and landsat-8 data. *International Archives of the Photogrammetry, Remote Sensing & Spatial Information Sciences*, *42*.

Tong, X., Brandt, M., Hiernaux, P., Herrmann, S., Rasmussen, L. V., Rasmussen, K., Tian, F., Tagesson, T., Zhang, W., & Fensholt, R. (2020). The forgotten land use class: Mapping of fallow fields across the sahel using sentinel-2. *Remote Sensing of Environment*, *239*, 111598.

Valero, S., Morin, D., Inglada, J., Sepulcre, G., Arias, M., Hagolle, O., Dedieu, G., Bontemps, S., Defourny, P., & Koetz, B. (2016). Production of a dynamic cropland mask by processing remote sensing image series at high temporal and spatial resolutions. *Remote Sensing*, *8*(1), 55.

Vancutsem, C., Marinho, E., Kayitakire, F., See, L., & Fritz, S. (2013). Harmonizing and combining existing land cover/land use datasets for cropland area monitoring at the african continental scale. *Remote Sensing*, *5*(1), 19–41.

Vintrou, E., Soumaré, M., Bernard, S., Bégué, A., Baron, C., & Lo Seen, D. (2012). Mapping fragmented agricultural systems in the sudano-sahelian environments of africa using random forest and ensemble metrics of coarse resolution modis imagery. *Photogrammetric Engineering & Remote Sensing*, *78*(8), 839–848.

Waldner, F., Fritz, S., Di Gregorio, A., & Defourny, P. R. S. (2015). Mapping priorities to focus cropland mapping activities: Fitness assessment of existing global, regional and national cropland maps. *Remote Sensing*, *7*(6), 7959–7986.

Weinmann, M., & Weidner, U. (2018). Land-cover and land-use classification based on multitemporal sentinel-2 data, In *Igarss 2018-2018 ieee international geoscience and remote sensing symposium*, IEEE.

Xiong, J., Thenkabail, P., Tilton, J., Gumma, M., Teluguntla, P., Oliphant, A., Congalton, R., Yadav, K., & Gorelick, N. (2017). Nominal 30-m cropland extent map of continental africa by integrating pixel-based and object-based algorithms using sentinel-2 and landsat-8 data on google earth engine. *Remote Sensing*, *9*(10), 1065.

Yang, N., Liu, D., Feng, Q., Xiong, Q., Zhang, L., Ren, T., Zhao, Y., Zhu, D., & Huang, J. (2019). Large-scale crop mapping based on machine learning and parallel computation with grids. *Remote Sensing*, *11*(12), 1500.